The Plant Cell, Vol. 27: 787–805, March 2015, www.plantcell.org

The bHLH Transcription Factor bHLH104 Interacts with IAA-LEUCINE RESISTANT3 and Modulates Iron Homeostasis in Arabidopsis

Jie Zhang,[1] Bing Liu,[1] Mengshu Li, Dongru Feng, Honglei Jin, Peng Wang, Jun Liu, Feng Xiong, Jinfa Wang, and Hong-Bin Wang[2]

State Key Laboratory of Biocontrol and Collaborative Innovation Center of Genetics and Development, Guangdong Provincial Key Laboratory of Plant Resources, School of Life Sciences, Sun Yat-sen University, 510275 Guangzhou, People's Republic of China

ORCID ID: 0000-0003-4957-0509 (H.-B.W.)

Iron (Fe) is an indispensable micronutrient for plant growth and development. The regulation of Fe homeostasis in plants is complex and involves a number of transcription factors. Here, we demonstrate that a basic helix-loop-helix (bHLH) transcription factor, bHLH104, belonging to the IVc subgroup of bHLH family, acts as a key component positively regulating Fe deficiency responses. Knockout of *bHLH104* in *Arabidopsis thaliana* greatly reduced tolerance to Fe deficiency, whereas overexpression of *bHLH104* had the opposite effect and led to accumulation of excess Fe in soil-grown conditions. The activation of Fe deficiency-inducible genes was substantially suppressed by loss of *bHLH104*. Further investigation showed that bHLH104 interacted with another IVc subgroup bHLH protein, IAA-LEUCINE RESISTANT3 (ILR3), which also plays an important role in Fe homeostasis. Moreover, bHLH104 and ILR3 could bind directly to the promoters of Ib subgroup *bHLH* genes and *POPEYE* (*PYE*) functioning in the regulation of Fe deficiency responses. Interestingly, genetic analysis showed that loss of *bHLH104* could decrease the tolerance to Fe deficiency conferred by the lesion of *BRUTUS*, which encodes an E3 ligase and interacts with bHLH104. Collectively, our data support that bHLH104 and ILR3 play pivotal roles in the regulation of Fe deficiency responses via targeting Ib subgroup *bHLH* genes and *PYE* expression.

INTRODUCTION

Iron (Fe) is a necessary micronutrient for both plants and animals. It is required as an essential cofactor for a number of cellular enzymatic reactions, such as photosynthesis, mitochondrial respiration, hormone biosynthesis, and nitrogen fixation (Hänsch and Mendel, 2009). Although Fe is one of the most abundant elements on earth, it often exists as insoluble ferric hydroxides in neutral and basic soils, resulting in low Fe bioavailability. Therefore, it is critical to determine the mechanisms underlying the uptake and trafficking of Fe, which is vital to improve Fe bioavailability and content of crops.

To optimize the Fe acquisition from soil, plants have evolved two major strategies to take up Fe: the reduction-based strategy (Strategy I) in dicotyledonous plants and nongraminaceous monocots, and the chelation-based strategy (Strategy II) specific to graminaceous monocots (Walker and Connolly, 2008; Hindt and Guerinot, 2012). Strategy I involves the extrusion of protons to decrease the pH of rhizosphere and the reduction of Fe^{3+} by FERRIC REDUCTASE OXIDASE2 (FRO2) to more soluble Fe^{2+}, which are subsequently imported across the root epidermal cell membrane via IRON REGULATED TRANSPORTER1 (IRT1) (Curie and Briat, 2003; Hell and Stephan, 2003); while the graminaceous monocots release phytosiderophores, such as mugineic acids, to chelate Fe from Fe-limited soil (Kobayashi et al., 2010).

Due to the important biological functions and special redox properties of Fe, plants have developed a series of sophisticated regulatory systems at transcriptional and posttranscriptional levels to maintain Fe homeostasis. A number of transcription factors involved in Fe homeostasis have been identified. In *Arabidopsis thaliana*, two regulatory networks, the FER-LIKE IRON DEFICIENCY-INDUCED TRANSCRIPTION FACTOR (FIT) network and the POPEYE (PYE) network, were verified to modulate Fe deficiency responses (Ivanov et al., 2012). Both FIT and PYE are members of the basic helix-loop-helix (bHLH) transcription factor family, suggesting the importance of bHLH proteins in Fe homeostasis. FIT was identified via its ortholog FER in tomato (*Solanum lycopersicum*) (Ling et al., 2002; Colangelo and Guerinot, 2004; Yuan et al., 2005; Bauer et al., 2007). The *FIT*-null mutation, *fit-1*, is lethal at the seedling stage without extra Fe supply, and approximately half of the Fe deficiency-inducible genes are deregulated in *fit-1* Fe-deficient roots (Colangelo and Guerinot, 2004). However, overexpression of *FIT* had no effect on the expression of its targets *FRO2* and *IRT1*, since their induction depends upon the dimerization of FIT with other four Ib subgroup bHLH proteins, bHLH38, bHLH39, bHLH100, and bHLH101, whose expression is dramatically induced by low Fe stress and repressed under Fe overload (Yuan et al., 2008; Wang et al., 2013b). These four Ib *bHLH* genes are induced independently from *FIT*, and the regulatory mechanism that acts upon *FIT* and Ib subgroup *bHLH* genes remains unclear.

The second regulatory system for Fe deficiency responses is mediated by the PYE bHLH protein, which is specifically induced in root pericycle under Fe-deficient conditions. The *pye-1* mutant is

[1] These authors contributed equally to this work.
[2] Address correspondence to wanghb@mail.sysu.edu.cn.
The author responsible for distribution of materials integral to the findings presented in this article in accordance with the policy described in the Instructions for Authors (www.plantcell.org) is: Hong-Bin Wang (wanghb@mail.sysu.edu.cn).
www.plantcell.org/cgi/doi/10.1105/tpc.114.132704

sensitive to Fe deficiency, and three Fe transport-related genes, *NA SYNTHASE4* (*NAS4*), *FRO3*, and *ZINC-INDUCED FACILITATOR1* (*ZIF1*), are highly upregulated under Fe-deficient conditions in *pye-1* mutant and identified as direct targets of PYE (Long et al., 2010). Additionally, a yeast two-hybrid assay showed that PYE can interact with IAA-LEUCINE RESISTANT3 (ILR3), which is also a bHLH transcription factor and may mediate metal homeostasis by regulating transporter levels (Rampey et al., 2006). In rice (*Oryza sativa*), a set of bHLH transcription factors have also been demonstrated to regulate Fe homeostasis. A homolog of Arabidopsis bHLH38 and bHLH39 in rice, IRON-RELATED TRANSCRIPTION FACTOR2 (IRO2), is essential for positively regulating genes involved in mugineic acid biosynthesis under Fe deficiency, and overexpression of *IRO2* improved both Fe uptake and translocation to seeds (Ogo et al., 2006, 2007, 2011). Moreover, a PYE homologous protein in rice, IRO3, is induced 20- to 70-fold upon Fe deficiency. *IRO3*-overexpressing lines are hypersensitive to low Fe, and the genes induced by Fe deficiency are inhibited in these plants, suggesting that IRO3 is a negative regulator of Fe deficiency responses in rice (Zheng et al., 2010). Recently, rice bHLH133 was characterized to play a role in the regulation of Fe transportation from roots to shoots, further demonstrating the roles for bHLH proteins in Fe homeostasis (Wang et al., 2013a).

Despite the fact that plants are frequently challenged by Fe deficiency, Fe can be toxic by generating hydroxyl radicals via the Fenton reaction when it is accumulated at high levels (Thomine and Vert, 2013). Two pea (*Pisum sativum*) mutants, *bronze* and *degenerative leaves*, were the first mutants identified to be able to accumulate excess Fe in plants, causing leaf bronzing or degeneration. However, the causative genes have not been identified (Grusak et al., 1990; Kneen et al., 1990). In Arabidopsis, knockdown of the phloem-specific Fe transporter OLIGOPEPTIDE TRANSPORTER3, which loads Fe into the phloem to regulate shoot-to-root signaling, leads to Fe overload in most organs of the plants, except in embryos (Stacey et al., 2008; Mendoza-Cózatl et al., 2014; Zhai et al., 2014). Recently, the lesion mutant of *SHK1 BINDING PROTEIN1*, which mediates symmetric histone dimethylation, was found to accumulate high levels of Fe in shoots and exhibit tolerance to Fe deficiency. This reveals that epigenetic control is involved in Fe homeostasis (Fan et al., 2014). By coexpression analysis of *PYE*, Long et al. (2010) found the E3 ligase BRUTUS (BTS) as a putative negative regulator of Fe absorption. The knockdown mutant of *BTS* shows increased tolerance compared with the wild type on Fe-deficient media (Long et al., 2010). BTS possesses three putative hemerythrin domains, which were reported to contain μ-oxo diiron centers that could reversibly bind O_2, functioning as metal storage or O_2 transport proteins (Wirstam et al., 2003). In mammals, the E3 ubiquitin ligase F-BOX AND LEUCINE-RICH REPEAT PROTEIN5 (FBXL5) was characterized to harbor a hemerythrin domain and promote Fe-dependent ubiquitination and degradation of IRON REGULATORY PROTEIN2 (Salahudeen et al., 2009; Vashisht et al., 2009). Most recently, knockdown of rice HEMERYTHRIN MOTIF-CONTAINING RING- AND ZINC-FINGER PROTEIN1 (HRZ1) or HRZ2, the orthologs of BTS, caused increased accumulation of Fe and enhanced tolerance to Fe deficiency (Kobayashi et al., 2013). These results further suggest a role for BTS in negatively regulating Fe acquisition in Arabidopsis.

In this study, we characterized an Arabidopsis transcription factor belonging to the IVc subgroup of bHLH family, bHLH104, which plays an important role in Fe homeostasis. Mutation of *bHLH104* led to significantly reduced tolerance to Fe deficiency, while overexpression of *bHLH104* strongly promoted Fe accumulation. Besides bHLH104, another IVc subgroup bHLH transcription factor, ILR3, was also found to be required for Fe deficiency responses and could form heterodimers with bHLH104. Chromatin immunoprecipitation (ChIP) assays demonstrated that bHLH104 and ILR3 regulated the expression of four Ib subgroup *bHLH* genes and *PYE* by binding to specific elements in their promoters, indicating a cascade of bHLH transcription factors during the control of Fe homeostasis. Further genetic analysis suggested that bHLH104 might function in the same pathway of BTS in Fe signaling.

RESULTS

The *bHLH104* Knockout Mutant Plants Have Altered Fe Homeostasis

Previous studies have shown that the regulation of genes that control Fe uptake and distribution by transcription factors such as bHLH family proteins is crucial for Fe homeostasis (Walker and Connolly, 2008; Hindt and Guerinot, 2012). Members in the IVc subgroup of bHLH transcription factor family were reported to interact with Fe deficiency response regulator PYE (Long et al., 2010), suggesting a putative role of this bHLH subgroup (bHLH34, bHLH104, ILR3, and bHLH115) in Fe homeostasis regulation. Thus, we screened several T-DNA insertion lines of these genes from the ABRC; however, only homozygous mutants of *bHLH104*, one harboring a T-DNA in the third intron (*bhlh104-1*), the other in the last exon (*bhlh104-2*), were identified as null mutants, exhibiting loss of the full-length *bHLH104* transcript (Figures 1A and 1B). Interestingly, when these *bhlh104* mutants were grown on the Fe-limited media (−Fe, without Fe; −Fe+Frz, with 50 μM ferrozine to chelate the trace amounts of Fe from agar), they showed an extreme inhibition of root growth and smaller, chlorotic cotyledons compared with larger and light-green cotyledons of the wild type. By contrast, when Fe was present at normal concentrations (+Fe, with 100 μM Fe), both *bhlh104-1* and *bhlh104-2* had no discernable differences from the wild type (Figure 1C). It is noteworthy that during the first few days, the growth of wild-type and *bhlh104* plants showed no obvious difference upon Fe deficiency. However, from the fifth day, the root growth of *bhlh104* mutants was significantly repressed and almost stopped at 1 week on Fe-deficient media with ferrozine (Supplemental Figure 1A). This might be due to the fact that the initial nutrition for the growth of *bhlh104* mutants came from the embryos, which did not rely on the exogenous Fe supply. In parallel, plants were first cultivated on Fe-sufficient media for 4 d and then exposed to Fe deficiency. Consistent with the results above, the leaves of *bhlh104* mutants became more chlorotic than the wild type 10 d after transfer (Supplemental Figure 1B). Besides of Fe deficiency, we also tested the response of *bhlh104* mutants to Zn, Cu, and Mn deficiency. The mutants displayed no observable phenotype under these stresses, indicating that the susceptibility of *bhlh104* mutants to Fe deficiency was specific (Supplemental Figure 1C).

We then investigated the H^+-ATPase activity and ferric-chelate reductase activity in *bhlh104* plants, which are typical indicators of Fe deprivation (Yi and Guerinot, 1996; Fox and Guerinot, 1998). Seven-day-old seedlings grown under Fe-sufficient or Fe-deficient conditions were tested by their rhizosphere acidification. As expected, the wild-type plants showed visible coloration around roots caused by activation of H^+-ATPase under Fe deficiency. By contrast, the *bhlh104* roots displayed an obvious decrease in acidification (Figure 1D). In addition, the ferric-chelate reductase activity was increased in both wild-type and *bhlh104* roots in response to Fe deficiency; however, the activity in the *bhlh104* mutants was decreased compared with the wild type (Figure 1E). These results indicated a defect in the Strategy I response due to the loss of *bHLH104*. To assess the Fe contents in wild-type and *bhlh104* plants, inductively coupled plasma-atomic emission spectrometry was used to quantify the Fe contents in shoots. In accordance with the inferior growth of *bhlh104* plants under Fe-deficient conditions, their shoots showed ~70% Fe relative to the wild type (Figure 1F). Furthermore, we also did Perls Fe staining in roots of wild-type and *bhlh104* plants. Similarly strong Fe staining was seen between them under Fe-sufficient conditions in which Fe was abundant in their roots; however, no signal was observed in their Fe-deficient roots. We noted that the root cells of *bhlh104* Fe-deficient plants showed no obvious alterations compared with the wild type, indicating that the reduced growth of *bhlh104* roots was not caused by inhibition of cell elongation (Supplemental Figure 1D).

We next examined the phenotypes of soil-grown *bhlh104* mutants. A slight chlorosis was observed in the young leaves of *bhlh104* plants at the time of bolting when grown in normal soil (Figure 1G). Fe content measurements revealed that the young leaves of *bhlh104* mutants showed 15.5% lower Fe levels than those in the wild type, whereas the adult leaves had similar Fe levels to the wild type (Figure 1G). We then germinated the plants in alkaline soil (pH 7 to 8), which makes Fe prone to form ferric hydroxides that cannot be easily used by plants (Guerinot and Yi, 1994). After growth for 2 weeks, the *bhlh104* mutants showed overall growth arrest, with only two pieces of bleached true leaves (Figure 1H). Taken together, these results suggest that *bHLH104* is crucial for the efficient uptake of Fe under Fe deficiency.

bHLH104-Overexpressing Plants Exhibit Increased Tolerance to Fe Deficiency

The physiological role of bHLH104 in Fe homeostasis was further investigated by analyzing the phenotypes of *bHLH104*-overexpressing (*bHLH104* ox) plants, in which a 35S promoter drove the expression of a *bHLH104-GFP* fusion gene. This tagged version could complement *bhlh104-2* mutants, indicating that the GFP tag did not interfere with the function of bHLH104 (Supplemental Figure 2). Three independent *bHLH104* ox lines were chosen for subsequent analyses by detecting fusion protein expression (Figure 2A). In contrast to the *bhlh104* mutants, the *bHLH104* ox plants showed significant tolerance of Fe-deficient (−Fe+Frz) media, with almost 2-fold root length and larger, greener leaves than the wild type (Figure 2B; Supplemental Figure 3A). The total chlorophyll content of the *bHLH104* ox plants was higher than that of the wild type under Fe-deficient conditions (Figure 2C). To determine whether *bHLH104* ox plants altered their H^+-ATPase and ferric-chelate reductase activities in response to Fe deficiency, we also detected rhizosphere acidification and conducted ferrozine assays. When cultivated under Fe-deficient conditions, the *bHLH104* ox plants exhibited obvious coloration around the roots more than the wild type, indicating increased H^+-ATPase activity with overexpression of *bHLH104* during Fe deficiency responses. By contrast under normal conditions, no distinct coloration was observed in the wild-type and *bHLH104* ox plants, which suggested that the H^+-ATPase activity of *bHLH104* ox plants was not constitutively activated, irrespective of Fe supply (Figure 2D). Furthermore, the ferric-chelate reductase activity of *bHLH104* ox roots was also higher under Fe deficiency and displayed a slight increase under Fe-sufficient conditions compared with the wild type (Figure 2E). Taken together, these results further indicated a positive role of *bHLH104* in Fe deficiency responses.

Overexpression of *bHLH104* Leads to Fe Overload under Normal Soil Cultivation

Due to the strikingly enhanced tolerance of *bHLH104* ox plants under conditions of Fe deficiency, we wondered whether growth features were altered in *bHLH104* ox plants under soil cultivation. Within the 4-week vegetative growth period of *bHLH104* ox plants in normal soil, no macroscopic alterations in phenotype were observed. However, around 2 weeks after bolting, a portion of siliques in *bHLH104* ox plants, especially those located at the bottom of the stem, appeared to be aborted. Furthermore, necrotic lesions were seen at the ends of the cauline leaves of *bHLH104* ox plants (Figures 3A and 3B). These necrotic lesions were verified by Trypan blue staining to detect cell death (Supplemental Methods). Strong staining was clearly observed where the hydathodes were localized and also at the end of the vasculature (Supplemental Figures 3B to 3G). These toxic symptoms prompted us to detect the location of Fe in *bHLH104* ox plants compared with the wild type using Perls staining. As shown in Figure 3, the rosette leaves of the wild type did not show detectable amounts of Fe^{3+} staining, whereas the *bHLH104* ox leaves exhibited high levels of Fe^{3+} along the margins, especially in the hydathodes (Figures 3C and 3D). Moreover, high levels of stainable Fe were also observed in the trichomes of *bHLH104* ox leaves (Figures 3E and 3F). Similar to the rosette leaves, the cauline leaves of *bHLH104* ox plants exhibited strong Fe^{3+} staining (Figures 3G and 3H) and the reproductive tissues of *bHLH104* ox plants also possessed more Fe^{3+} than their counterparts in the wild type. As with leaves, the wild type had no detectable Fe^{3+} in the flowers; by contrast, large amounts of Fe^{3+} were observed in the sepals of *bHLH104* ox flowers (Figures 3I and 3J). To investigate whether the Fe overaccumulation resulted in abortion of siliques, we performed Fe^{3+} staining in mature siliques and aborted siliques of *bHLH104* ox plants, respectively. Interestingly, the mature siliques had detectable Fe^{3+} only in their distal ends, while significant Fe staining was observed throughout the aborted siliques (Figures 3K to 3N), which hinted that the abortion likely resulted from Fe toxicity. This Fe overaccumulation was also reflected by significantly higher transcript levels of *FERRETIN1* (*FER1*), encoding one of the ferritin isoforms, in *bHLH104* ox leaves, flowers, and seeds compared with the wild type (Figure 3O), supporting the view that ferritin

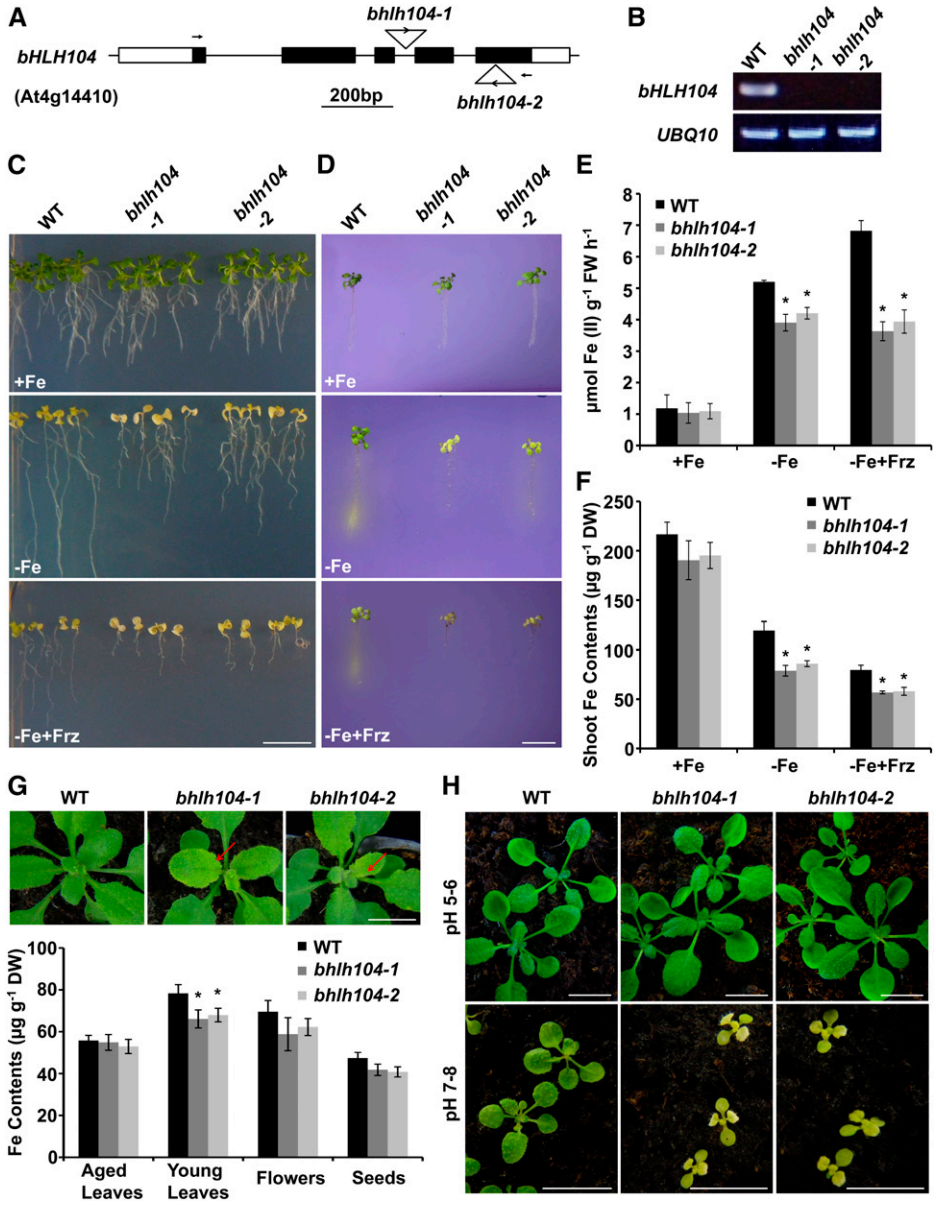

Figure 1. The *bHLH104* Knockout Mutants Have Decreased Tolerance to Fe-Deficient Conditions.

(A) The position and orientation of the T-DNA insertion site for *bhlh104-1* (Salk_099496C) and *bhlh104-2* (Salk_043862C) mutants.
(B) Testing for the full-length *bHLH104* transcript in the wild type and the *bhlh104-1* and *bhlh104-2* mutants grown for 4 weeks in normal soil by RT-PCR. Primers used for amplification of *bHLH104* are indicated in **(A)**. Amplification of *UBIQUITIN10* (*UBQ10*) is shown as a control.
(C) Phenotypes of the wild type and the *bhlh104* mutants grown for 2 weeks on Fe-sufficient (+Fe, 100 μM Fe) or Fe-deficient (−Fe, without Fe; −Fe +Frz, with 50 μM ferrozine) media. Bar = 1 cm.
(D) Rhizosphere acidification by 7-d-old wild type and *bhlh104* mutants grown on Fe-sufficient (+Fe) or Fe-deficient (−Fe and −Fe+Frz) media. Four plants were transferred to agar plates containing bromocresol purple for 24 h. Acidification is indicated by a yellow color around the roots. Bar = 1 cm.
(E) Ferric-chelate reductase activity of the wild type and *bhlh104* mutants grown on Fe-sufficient (+Fe) or Fe-deficient (−Fe and −Fe+Frz) media for 7 d. The ferrozine assay was performed on 10 pooled plant roots. Values are means ± SD of three independent experiments. Significant differences from the wild type are indicated by an asterisk ($P < 0.05$), as determined by Student's *t* test. FW, fresh weight.
(F) Fe contents in shoots of plants grown on Fe-sufficient (+Fe) or Fe-deficient (−Fe and −Fe+Frz) media for 8 d. The data represent means ± SD of three independent experiments. Significant differences from the wild type are indicated by an asterisk ($P < 0.05$), as determined by Student's *t* test. DW, dry weight.
(G) Representative images of the wild type and *bhlh104* mutants grown in normal soil for 25 d. Arrows indicate slight chlorosis in young leaves of *bhlh104* plants compared with the wild type. Below the leaf graphs are the Fe contents in rosette leaves, flowers, and seeds of the wild type and *bhlh104* mutants. For 4-week-old plants, aged leaves refer to the third true leaf to the sixth leaf, while young leaves refer to the seventh leaf to the tenth

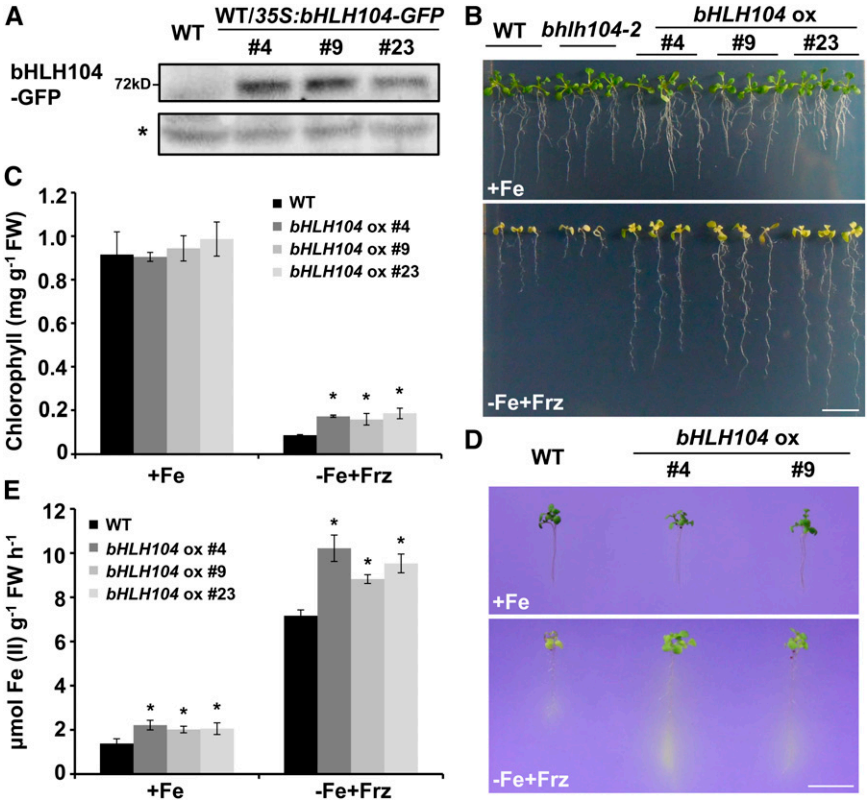

Figure 2. Plants Overexpressing *bHLH104* Exhibit Enhanced Tolerance to Fe Deficiency.

(A) The level of the bHLH104-GFP fusion protein in shoots of 7-d-old *bHLH104* ox plants grown on half-strength MS media, as determined by immunoblot analysis using an anti-GFP antibody. The asterisk labels the nonspecific signal used as loading control.
(B) Phenotypes of wild-type and *bHLH104* ox plants grown for 2 weeks on Fe-sufficient (+Fe) or Fe-deficient (−Fe+Frz) media. Bar = 1 cm.
(C) Total chlorophyll contents in wild-type and *bHLH104* ox plants grown for 2 weeks on Fe-sufficient (+Fe) or Fe-deficient (−Fe+Frz) media. The data represent means ± SD of three independent experiments. Significant differences from the wild type are indicated by an asterisk ($P < 0.05$), as determined by Student's *t* test.
(D) Rhizosphere acidification of 7-d-old wild-type and *bHLH104* ox plants grown on Fe-sufficient (+Fe) or Fe-deficient (−Fe+Frz) media. Bar = 1 cm.
(E) Ferric-chelate reductase activity of wild-type and *bHLH104* ox plants grown on Fe-sufficient (+Fe) or Fe-deficient (−Fe+Frz) media for 7 d. The data represent means ± SD of three independent experiments. Significant differences from the wild type are indicated by an asterisk ($P < 0.05$), as determined by Student's *t* test.

functions in protecting cells against oxidative damage resulting from Fe overload (Ravet et al., 2009).

To study the Fe distribution in leaves in more detail, Perls staining and diaminobenzidine (DAB) intensification assays were conducted on cross sections of leaves. It was remarkable that there were Fe deposits in the phloem of both young and aged leaves of *bHLH104* ox plants, whereas no signal was observed in the wild type (Figure 3P). This indicates that the excessively absorbed Fe may be retained in the phloem and could not be employed by mesophyll cells; thus, the phloem appears to be an important tissue for Fe transport. Taken together, overexpression of *bHLH104* results in overaccumulation of Fe in various organs of plants and the excess Fe in the vasculature is mainly enriched in the phloem.

Expression of Genes Responding to Fe Deficiency Is Regulated by bHLH104

Changes in Fe availability could release signals to regulate the expression of genes involved in Fe acquisition and transport

Figure 1. (continued).

leaf. Rosette leaves and flowers were harvested at 1 week after bolting. The results are means ± SD of three independent experiments. Significant differences from the wild type are indicated by an asterisk ($P < 0.05$), as determined by Student's *t* test. Bar = 1 cm.
(H) Phenotypes of 3-week-old wild type and *bhlh104* mutants germinated on either normal soil (pH 5 to 6) or alkaline soil (pH 7 to 8). Bars = 1 cm.

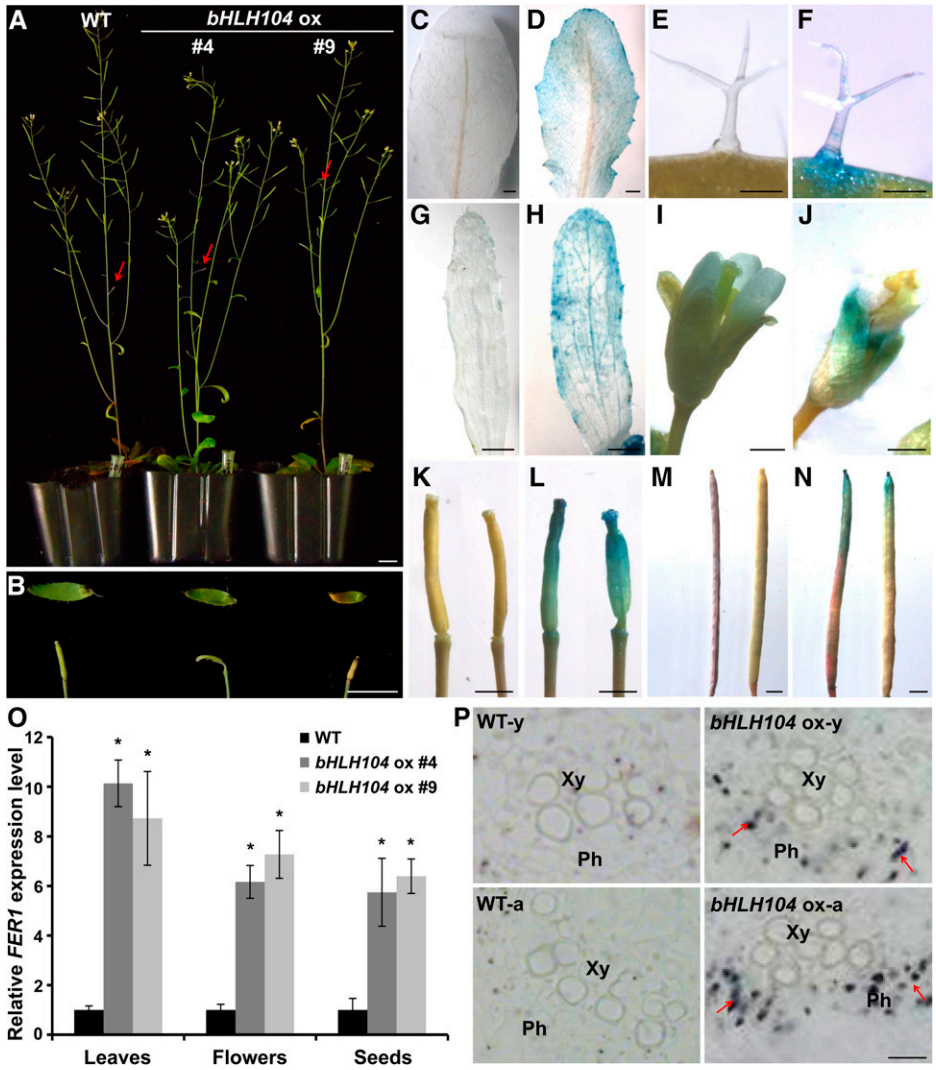

Figure 3. Overexpression of *bHLH104* Results in Fe Overaccumulation in Soil Growth Conditions.

(A) Phenotypes of wild-type and *bHLH104* ox plants at the reproductive stage. Bar = 1 cm.
(B) Magnified image of cauline leaves and siliques (marked by arrowheads in **[A]**) in wild-type and *bHLH104* ox plants. Bar = 500 μm.
(C) to **(N)** Perls Fe stain signals in rosette leaves (**[C]** and **[D]**), trichomes (**[E]** and **[F]**), cauline leaves (**[G]** and **[H]**), flowers (**[I]** and **[J]**), young siliques (**[K]** and **[L]**), and mature siliques (**[M]** and **[N]**) of wild-type (**[C]**, **[E]**, **[G]**, **[I]**, **[K]**, and **[M]**) and *bHLH104* ox (**[D]**, **[F]**, **[H]**, **[J]**, **[L]**, and **[N]**) plants. Bars = 1 mm in **(C)**, **(D)**, **(G)**, **(H)**, and **(K)** to **(N)**, 100 μm in **(E)** and **(F)**, and 500 μm in **(I)** and **(J)**.
(O) The relative expression of *FER1* in wild-type and *bHLH104* ox leaves, flowers, and seeds. Plants were grown for 6 weeks in soil. The gene expression level in the wild type was set to 1. The data represent means ± SD of three independent experiments. Significant differences from the corresponding wild type are indicated by an asterisk ($P < 0.05$), as determined by Student's *t* test.
(P) Perls/DAB stain for Fe^{3+} signals in 4-μm cross sections of wild-type and *bHLH104* ox young (Y) and aged (A) leaves, showing Fe deposits in phloem of the vessels in *bHLH104* ox plants (indicated by arrows). Ph, phloem; Xy, xylem. Bar = 10 μm.

(Thimm et al., 2001). To examine the effect of *bHLH104* deletion or overexpression on the regulation of genes related to Fe deficiency, several representative genes were selected for analysis under Fe-sufficient (+Fe) and Fe-deficient (−Fe+Frz) conditions using quantitative real-time PCR (qPCR). As shown in Table 1, the expression of *bHLH34* and *ILR3* did not show significant differences among these plants under both conditions, while *bHLH115* showed a 2-fold induction upon Fe deficiency; however, this expression was not affected by loss or overexpression of *bHLH104.* These indicated that the level of *bHLH104* did not influence the expression of other three IVc subgroup *bHLH* genes. The expression of Fe uptake machinery genes, *FIT*, *FRO2*, and *IRT1*, whose transcript abundance could be induced by low Fe (Robinson et al., 1999; Vert et al., 2002; Colangelo and Guerinot, 2004), was limited in *bhlh104* mutants. Moreover, the upregulated expression of four subgroup Ib *bHLH* genes under Fe-deficient conditions (Wang et al., 2007; Sivitz

et al., 2012) was dramatically suppressed in *bhlh104* plants. In addition, under Fe-sufficient conditions, the expression levels of these four genes in *bhlh104* mutants were also lower than the wild type, with ~2-fold reduction. Induction of *PYE* and *BTS* by Fe deficiency, which is considered to represent another pathway that regulates Fe utilization (Long et al., 2010), was also lower in the *bhlh104* mutants compared with the wild type. In addition, the expression levels of Fe transport-related genes, such as *NAS4*, *FERRIC REDUCTASE DEFECTIVE3* (*FRD3*), and *ZIF1* (Green and Rogers, 2004; Haydon and Cobbett, 2007; Klatte et al., 2009), were all deregulated by the loss of *bHLH104*.

By contrast, the expression of these Fe uptake- and transport-related genes in *bHLH104* ox plants was upregulated compared with the wild type under both Fe-sufficient and Fe-deficient conditions (Table 1). Based on these expression analyses for Fe-related genes, it appears that bHLH104 functions relatively upstream in the transcriptional regulatory network of the Fe deficiency response.

bHLH104 Interacts with Another IVc Subgroup bHLH Transcription Factor ILR3

The IVc subgroup of bHLH transcription factor comprises four members, bHLH34, bHLH104, ILR3, and bHLH115. Given the potential for bHLH transcription factors to regulate the expression of downstream genes by forming diverse homodimers or heterodimers (Toledo-Ortiz et al., 2003), we then tested whether bHLH104 interacted with members of IVc subgroup bHLH transcription factors and other known bHLH proteins involved in the Fe homeostasis regulation using bimolecular fluorescence complementation (BiFC) assays. As shown in Figure 4A, bHLH104 showed no signal with Ib subgroup bHLH transcription factors or FIT. However, bHLH104 could interact with itself and bind strongly to ILR3, which was suggested to be involved in the regulation of metal homeostasis in a previous study (Rampey et al., 2006). Moreover, bHLH104 also showed an intense interaction with bHLH115, which shares 63% similarity with ILR3. We also observed a slight signal between bHLH104 and bHLH34, as well as with PYE. These results imply that bHLH104 may function with other members of IVc subgroup bHLH transcription factors, but not with Ib subgroup bHLH proteins. To further confirm the interaction of bHLH104 with ILR3 and bHLH115, a glutathione *S*-transferase (GST) pull-down assay was performed using a recombinant N-terminal GST-tagged bHLH104 protein. As shown in Figure 4B, the GFP-tagged ILR3 and bHLH115 protein could be pulled down by GST-bHLH104, but not by GST alone, indicating that bHLH104 interacts with ILR3 and bHLH115 in vitro. Consistent with the results of the pull-down assay, an in vivo coimmunoprecipitation (co-IP) assay also showed that bHLH104-Flag fusion proteins could be immunoprecipitated with ILR3-GFP or bHLH115-GFP when they were transiently coexpressed in Arabidopsis protoplasts (Figure 4C). These results indicate that bHLH104 may

Table 1. Differential Expression of Fe Deficiency-Responsive Genes in Roots of the Wild Type, *bhlh104* Mutants, and *bHLH104* ox Plants

	+Fe Roots				−Fe+Frz Roots				
Genes	*bhlh104-1*	*bhlh104-2*	*bHLH104* ox#4	*bHLH104* ox#9	Wild Type	*bhlh104-1*	*bhlh104-2*	*bHLH104* ox#4	*bHLH104* ox#9
Subgroup IVc *bHLH* genes									
bHLH104	0.04 ± 0.01*	0.05 ± 0.01*	6.56 ± 0.76*	6.82 ± 0.55*	1.12 ± 0.03	0.03 ± 0.01*	0.04 ± 0.01*	4.52 ± 0.58*	4.18 ± 0.84*
bHLH34	0.93 ± 0.11	0.99 ± 0.12	1.08 ± 0.11	0.96 ± 0.06	1.06 ± 0.08	0.92 ± 0.08	0.97 ± 0.15	0.89 ± 0.11	1.04 ± 0.06
ILR3	0.84 ± 0.08	1.06 ± 0.22	0.92 ± 0.07	1.05 ± 0.07	0.97 ± 0.04	0.88 ± 0.06	0.80 ± 0.15	1.06 ± 0.12	1.03 ± 0.15
bHLH115	0.97 ± 0.06	1.05 ± 0.12	1.24 ± 0.25	0.98 ± 0.08	1.85 ± 0.23	1.94 ± 0.26	1.89 ± 0.14	1.82 ± 0.20	1.65 ± 0.21
Subgroup Ib *bHLH* genes									
bHLH38	0.43 ± 0.07*	0.55 ± 0.03*	18.70 ± 2.75*	14.73 ± 3.92*	107.39 ± 9.63	33.59 ± 5.58*	20.71 ± 3.33*	128.91 ± 11.88	123.08 ± 7.84
bHLH39	0.39 ± 0.06*	0.42 ± 0.04*	12.25 ± 4.42*	14.62 ± 3.15*	46.85 ± 6.65	14.17 ± 3.06*	10.02 ± 2.11*	63.56 ± 6.86	65.80 ± 8.01
bHLH100	0.36 ± 0.05*	0.41 ± 0.06*	45.64 ± 7.60*	37.79 ± 5.82*	237.84 ± 25.49	58.08 ± 4.06*	34.89 ± 6.12*	376.12 ± 26.61	317.4 ± 19.52
bHLH101	0.37 ± 0.05*	0.45 ± 0.06*	161.24 ± 12.45*	186.33 ± 18.20*	52.90 ± 5.74	7.19 ± 1.64*	7.42 ± 0.44*	188.07 ± 10.97*	186.76 ± 15.54*
Fe uptake									
FIT	0.99 ± 0.06	1.15 ± 0.22	3.92 ± 0.62*	2.24 ± 0.45*	2.65 ± 0.68	2.17 ± 0.30	1.97 ± 0.49	8.29 ± 1.02*	8.20 ± 2.62*
FRO2	0.32 ± 0.04*	0.48 ± 0.07*	56.11 ± 7.70*	35.95 ± 9.52*	86.53 ± 7.56	31.17 ± 4.92*	25.15 ± 7.23*	183.26 ± 11.31*	172.45 ± 15.11*
IRT1	0.64 ± 0.09	0.61 ± 0.04	33.48 ± 6.46*	19.29 ± 5.57*	43.41 ± 7.99	16.97 ± 3.14*	13.27 ± 2.11*	72.26 ± 5.32*	62.54 ± 8.56
IRT2	1.11 ± 0.17	0.63 ± 0.06	1.58 ± 0.30	1.67 ± 0.38	1.41 ± 0.12	0.92 ± 0.08	0.88 ± 0.06	2.83 ± 0.58*	3.07 ± 0.82*
Fe translocation									
YSL1	1.28 ± 0.13	0.78 ± 0.10	27.20 ± 3.39*	22.43 ± 3.03*	0.22 ± 0.02	0.28 ± 0.08	0.42 ± 0.07	2.83 ± 0.54*	2.39 ± 0.32*
NAS4	0.94 ± 0.03	0.69 ± 0.10	45.77 ± 7.00*	90.25 ± 9.49*	84.66 ± 10.25	16.35 ± 3.57*	12.14 ± 2.5*	134.73 ± 11.01*	161.15 ± 15.94*
ZIF1	0.89 ± 0.03	1.21 ± 0.11	6.32 ± 0.52*	6.39 ± 0.89*	10.78 ± 1.50	3.09 ± 0.64*	2.18 ± 0.36*	18.09 ± 2.64*	16.51 ± 2.06*
FRD3	0.76 ± 0.07	0.87 ± 0.03	4.59 ± 0.34*	5.29 ± 0.60*	0.82 ± 0.10	0.17 ± 0.06*	0.22 ± 0.12*	1.41 ± 0.08*	2.36 ± 0.21*
Fe homeostasis regulation									
PYE	0.80 ± 0.06	0.78 ± 0.08	6.17 ± 1.14*	7.42 ± 0.96*	3.80 ± 0.83	1.76 ± 0.16*	1.36 ± 0.23*	9.09 ± 1.59*	9.16 ± 0.98*
BTS	1.06 ± 0.06	1.10 ± 0.06	3.06 ± 0.23*	3.29 ± 0.50*	7.26 ± 1.02	2.51 ± 0.37*	1.72 ± 0.22*	8.40 ± 2.54	9.07 ± 1.45
MYB10	0.87 ± 0.08	0.96 ± 0.10	13.60 ± 3.54*	12.09 ± 2.69*	40.88 ± 8.16	6.43 ± 1.54*	10.32 ± 1.48*	69.55 ± 4.94*	70.12 ± 8.32*
MYB72	0.46 ± 0.07*	0.74 ± 0.08	276.29 ± 28.85*	145.2 ± 19.31*	560.15 ± 37.18	44.03 ± 5.35*	55.63 ± 7.39*	1710.28 ± 90.73*	1525.01 ± 96.46*

The relative gene expression levels measured by qPCR in roots of the wild type, *bhlh104* mutants, and *bHLH104* ox plants grown on Fe-sufficient (+Fe) or Fe-deficient (−Fe+Frz) media for 8 d. The expression of *TUB2* was used to normalize mRNA levels, and the gene expression level in the wild type under Fe-sufficient conditions was set to 1. The data represent means ± SD of three independent experiments. Significant differences from the corresponding wild type are indicated by an asterisk ($P < 0.05$), as determined by Student's *t* test.

regulate Fe homeostasis by forming heterodimers with ILR3 and bHLH115.

ILR3 Also Functions in Response to Fe Deficiency in Arabidopsis

The interaction between bHLH104 and ILR3 raised the question of whether ILR3 was also required for the Fe deficiency responses. To this end, we examined the phenotype of an *ILR3* knockout mutant, *ilr3-2*, on Fe-deficient media. Furthermore, we identified a partial loss-of-function allele and named it *ilr3-3* (Figures 5A and 5B). Interestingly, both the *ilr3-2* and *ilr3-3* mutants displayed hypersensitivity on Fe-deficient (−Fe and −Fe+Frz) media, exhibiting chlorotic leaves and short roots, which seemed even more severe than the *bhlh104-1* plants (Figure 5C). These two *ilr3* mutants revealed interveinal chlorosis of young leaves under soil-growth conditions (Figure 5D), similar to the phenotype caused by Fe deficiency. We then analyzed the expression of several Fe deficiency-responsive genes in *ilr3-2* roots. Similar to the *bhlh104* mutants, the expression of Fe uptake genes, *FIT*, *FRO2*, and *IRT1*, as well as four Ib subgroup *bHLH* genes, all showed significant decrease in *ilr3-2* roots upon Fe deficiency, compared with the wild type (Figure 5E). The expression of *bHLH104* in *ilr3-2* showed no significant difference compared with that in the wild type under both conditions, indicating that the mutation of *ILR3* did not affect the expression of *bHLH104*. Taken together, these

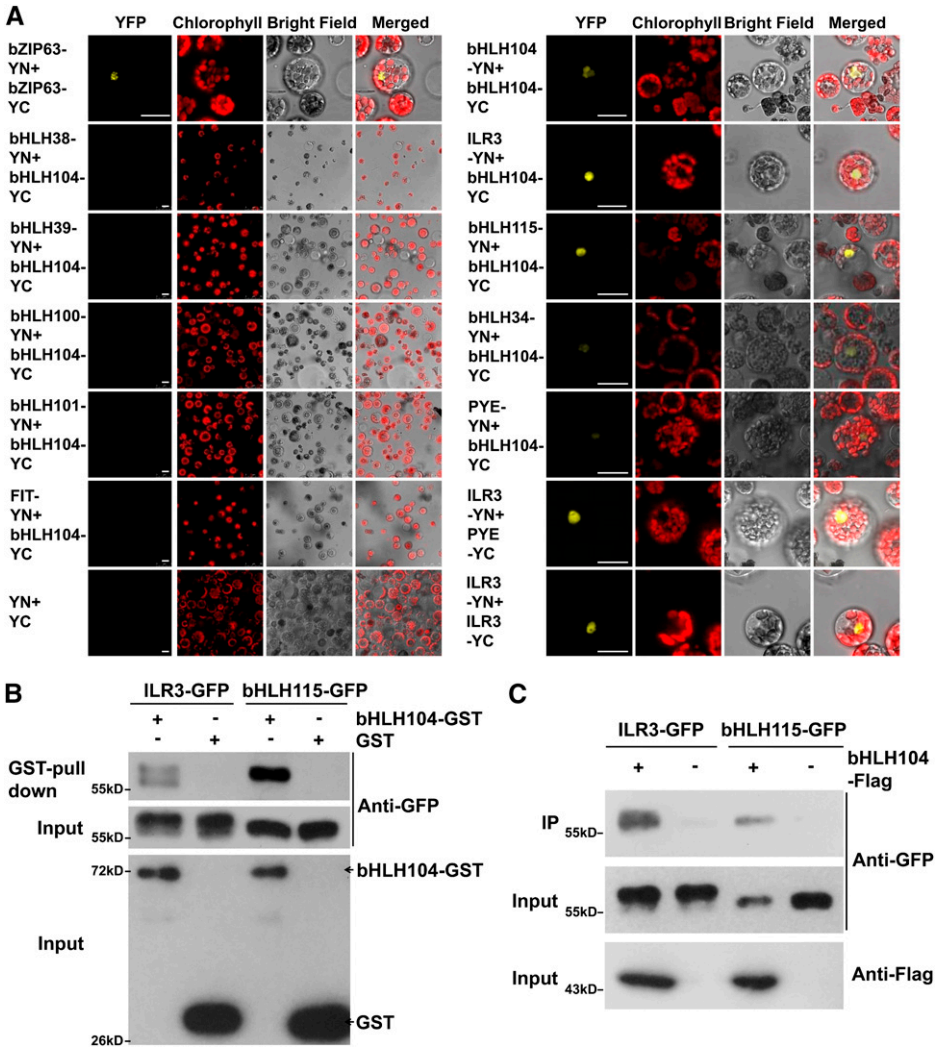

Figure 4. bHLH104 Interacts with Itself, ILR3, and bHLH115, but Not Ib Subgroup bHLH Proteins or FIT.

(A) BiFC analysis in Arabidopsis protoplasts transformed with different combinations of the constructs and visualized using confocal microscopy. Bars = 20 μm.

(B) Pull-down assay of GST-fused bHLH104 expressed in *Escherichia coli* with ILR3-GFP or bHLH115-GFP expressed in Arabidopsis protoplasts. Total proteins were pulled down by glutathione Sepharose 4B and detected using an anti-GFP antibody.

(C) Co-IP assay of bHLH104-Flag and ILR3-GFP or bHLH115-GFP coexpressed in Arabidopsis protoplasts. Total proteins were immunoprecipitated by anti-FLAG M2 affinity gel and detected using an anti-GFP antibody.

results suggest a critical role for ILR3 in the Fe deficiency responses.

Having ascertained that ILR3 is involved in Fe homeostasis regulation, we then asked whether *ILR3*-overexpressing plants also had enhanced resistance to Fe deficiency. As expected, plants overexpressing *35S:ILR3-GFP* (*ILR3* ox), in which ILR3 was fused to a GFP tag, displayed longer roots and more leaves than the wild type on Fe-deficient (−Fe+Frz) media (Figure 6A; Supplemental Figures 4A to 4C). Interestingly, *ILR3* ox plants showed small rosette and pale leaves compared with the wild type when grown in soil, with several leaves being chlorotic (Figure 6B). To further determine whether the *ILR3* ox plants showed a similar Fe distribution pattern to *bHLH104* ox plants, we localized Fe^{3+} in various organs of *ILR3* ox plants. As shown in the *bHLH104* ox plants, the rosette leaves of *ILR3* ox plants also possessed large quantities of Fe^{3+} in the vasculature (Figures 6C and 6D). Moreover, several necrotic spots were seen scattered in the leaves where Fe was overaccumulated (Figure 6E; Supplemental Figures 4D to 4G). Furthermore, the sepals of flowers and the aborted siliques which were also observed in *ILR3* ox plants

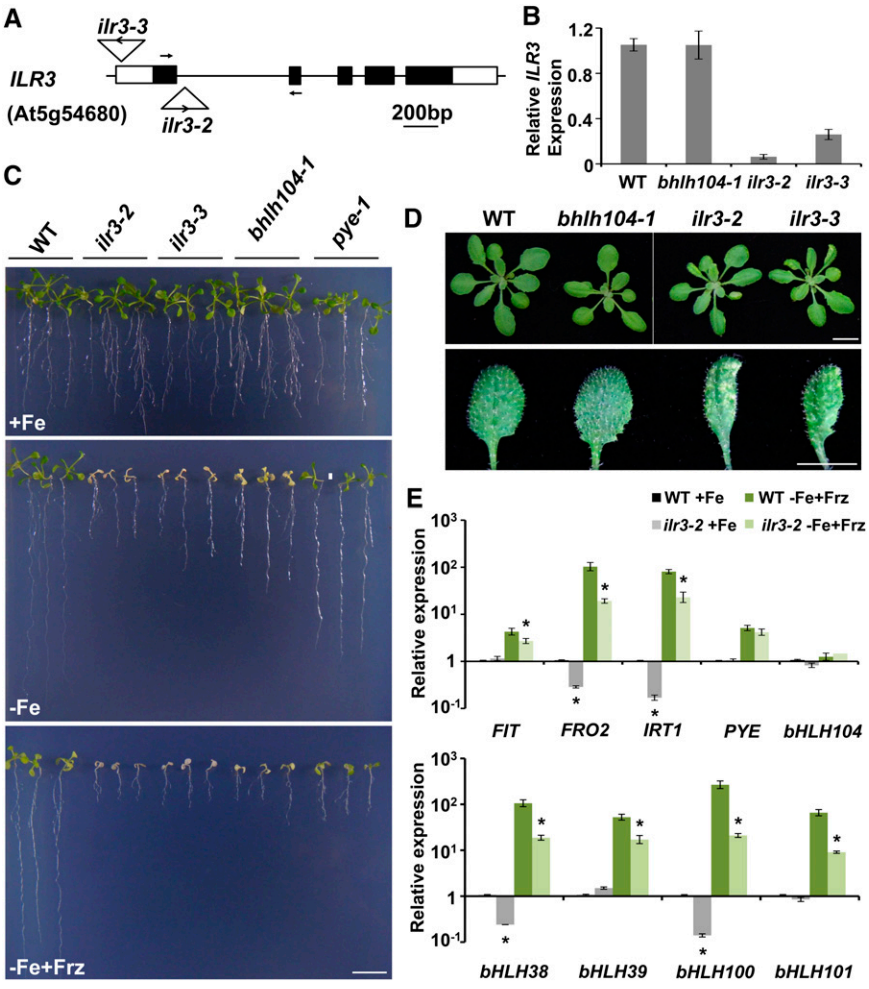

Figure 5. The *ILR3* Knockout Mutants Show Sensitivity to Fe Deficiency and Decreased Expression of Fe Uptake-Related Genes.

(A) The position and orientation of the T-DNA insertion site for the *ilr3-2* (Salk_004997C) and *ilr3-3* (Salk_043690C) mutants.

(B) Determination of the relative *ILR3* expression level in wild-type, *bhlh104-1*, *ilr3-2*, and *ilr3-3* plants grown for 4 weeks in normal soil, assessed by qPCR. Primers used for amplification of *ILR3* are indicated in **(A)**. Values are means ± SD of three independent experiments.

(C) Phenotype of wild-type, *ilr3-2*, *ilr3-3*, *bhlh104-1*, and *pye-1* mutants grown for 2 weeks on Fe-sufficient (+Fe) or Fe-deficient (−Fe and −Fe+Frz) media. Bar = 1 cm.

(D) Phenotypes of wild-type, *bhlh104*, and *ilr3* mutants grown in normal soil for 4 weeks. The magnified picture of leaves shows interveinal leaf chlorosis of *ilr3* mutants. Bars = 1 cm.

(E) The relative gene expression measured by qPCR in roots of wild-type and *ilr3-2* plants grown on Fe-sufficient (+Fe) or Fe-deficient (−Fe+Frz) media for 8 d. The expression of *TUB2* was used to normalize mRNA levels, and the gene expression level in the wild type under Fe-sufficient conditions was set to 1. The data represent means ± SD of three independent experiments. Significant differences from the corresponding wild type are indicated by an asterisk ($P < 0.05$), as determined by Student's *t* test.

accumulated extremely high levels of Fe (Figures 6F to 6I). Thus, consistent with *bHLH104* ox plants, overexpression of *ILR3* also gives rise to Fe overload in Arabidopsis.

bHLH104 and ILR3 Bind to the E-Box Motifs in the Promoters of Ib Subgroup *bHLH* Genes and *PYE*

The bHLH transcription factors have been reported to be associated with the E-box (5′-CANNTG-3′) *cis*-element in the promoters of their target genes (Fisher and Goding, 1992). Considering that *FIT* and four Ib subgroup *bHLH* genes were downregulated in *bhlh104* and *ilr3* mutants, we speculated whether these known *bHLH* genes were directly regulated by bHLH104 or ILR3. Bioinformatics analysis showed several E-box motifs were in the putative promoter regions of *FIT*, Ib subgroup *bHLH* genes, and *PYE* (Figure 7A). To determine the binding capacity of bHLH104 and ILR3 to their promoters, ChIP experiments were conducted. *35S:bHLH104-Flag* and *35S:ILR3-Flag* were transformed into Arabidopsis protoplasts, and ChIP DNA was immunoprecipitated using anti-FLAG affinity gel. A fragment of the *TUB2* promoter containing an E-box motif was used as a negative control. qPCR analyses showed that bHLH104 and ILR3 bound strongly to the promoters of Ib subgroup *bHLH* genes and *PYE*, but not to *FIT* (Figure 7B). Interestingly, the canonical E-box motifs (CACGTG, also referred to as G-box) in *bHLH38*, *bHLH100*, *bHLH101*, and *PYE* promoters were more enriched than their noncanonical E-box (CANNTG) motifs. However, bHLH104 and ILR3 could also recognize the chromatin region of the *bHLH39* promoter, which only harbors noncanonical E-box sequences (Figure 7B). These results indicate that bHLH104 and ILR3 interact with the specific E-box regulatory elements of Ib subgroup *bHLH* genes and *PYE* to affect their transcription during the response to Fe deficiency.

Loss of *bHLH104* Partially Rescues the Phenotype Conferred by *BTS* Lesion

It has been reported that bHLH104 and ILR3 could interact with BTS in a yeast two-hybrid assay; moreover, the phenotype of increased tolerance on Fe-deficient media was also seen in a partial loss-of-function allele *bts-1*, which has 70% *BTS* expression (Long et al., 2010). To further confirm the function of BTS in Fe homeostasis, we performed RNA interference of *BTS* and obtained transgenic lines with only 20% *BTS* expression (Supplemental Figure 5A). Furthermore, we also identified an Fe deficiency-tolerant mutant (Salk_004748C). Positional cloning of this mutant identified the *BTS* locus, whose first intron has a 47-bp fragment deletion, thus destroying its open reading frame (Figure 8A). This mutant also harbors a T-DNA in At1g67520 that encodes a putative lectin protein kinase. Using a segregating population, the T-DNA insertion in At1g67520 was separated and a homozygous mutation for *BTS* was obtained, namely, *bts-2*. We then investigated the responses of *BTS* RNA interference (RNAi) and *bts-2* plants to Fe deficiency. In accordance with the phenotype of *bts-1* mutant, the *BTS* RNAi and *bts-2* plants showed remarkably better growth on Fe-deficient (−Fe+Frz) media (Figures 8B and 8C; Supplemental Figure 5B). Moreover, the *BTS* RNAi and *bts-2* plants had significantly higher Fe contents in their rosette leaves, flowers, and seeds compared with the wild type (Figure 8D). Thus, our results reinforce the view that BTS functions as a negative regulator of the Fe deprivation response and Fe uptake.

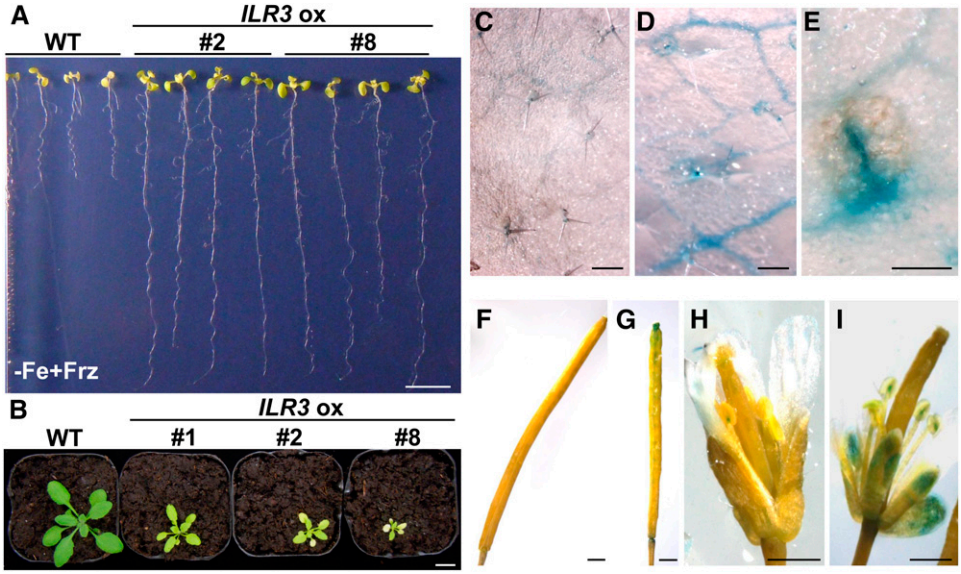

Figure 6. Plants Overexpressing *ILR3* Exhibit Enhanced Fe Deficiency Tolerance.

(A) Phenotypes of wild-type and *ILR3* ox plants grown for 2 weeks on Fe-deficient (−Fe+Frz) media. Bar = 1 cm.
(B) Phenotypes of wild-type and *ILR3* ox plants grown in normal soil for 4 weeks. Bar = 1 cm.
(C) to **(I)** Perls Fe stain signals in rosette leaves (**[C]** to **[E]**), siliques (**[F]** and **[G]**), and flowers (**[H]** and **[I]**) of wild-type (**[C]**, **[F]**, and **[H]**) and *ILR3* ox (**[D]**, **[E]**, **[G]**, and **[I]**) plants.
Bars = 200 μm in **(C)** to **(E)** and 1 mm in **(F)** to **(I)**.

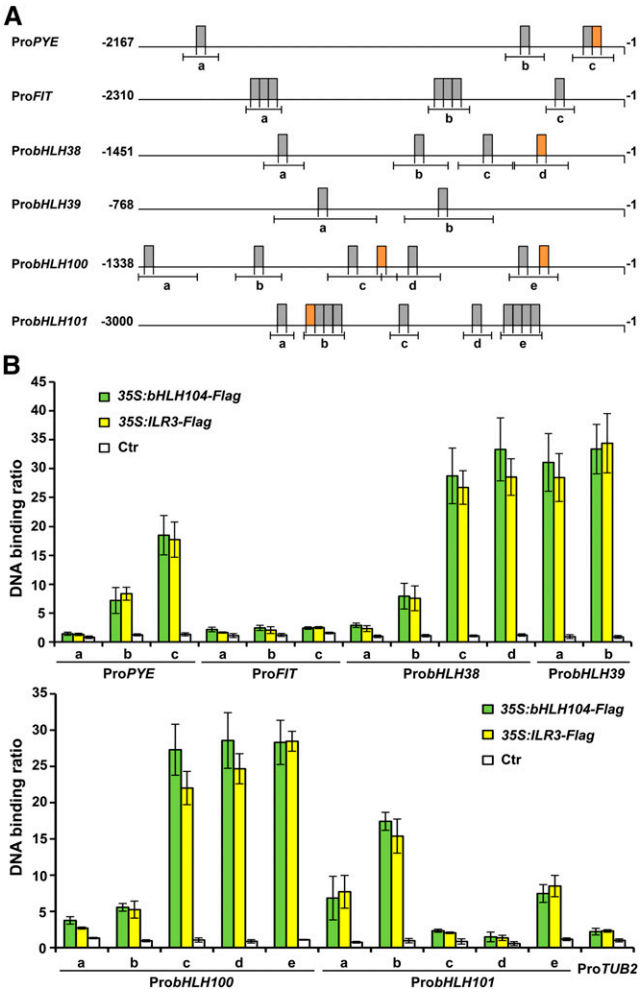

Figure 7. ChIP-qPCR Analyses of the Binding of bHLH104 and ILR3 to the Promoters of *PYE*, *FIT*, and Ib Subgroup *bHLH* Genes.

(A) Promoter structure diagrams for *PYE*, *FIT*, and Ib subgroup *bHLH* genes. Gray boxes show noncanonical E-boxes with sequence 5′-CANNTG-3′, while orange boxes show canonical E-boxes (5′-CACGTG-3′). Lines under the boxes indicate sequences detected by ChIP-qPCR assays.

(B) ChIP-qPCR analyses of the DNA binding ratio of bHLH104 and ILR3 to the promoters of *PYE*, *FIT*, and Ib subgroup *bHLH* genes. Chromatin from Arabidopsis protoplasts expressing *35S:bHLH104-Flag* or *35S:ILR3-Flag* was extracted by anti-FLAG M2 affinity gel. The protoplasts without transfection were used as negative control. qPCR was used to quantify enrichment of the *PYE*, *FIT*, and Ib subgroup *bHLH* gene promoters and a fragment of the *TUB2* promoter containing an E-box motif was used as a negative control. The binding of *TUB2* promoter fragment in protoplasts without transfection was set to 1 and used to normalize the DNA binding ratio of *bHLH* genes. The data represent means ± SD of three independent experiments.

We also tested the phenotype of *BTS* RNAi plants under normal soil cultivation. During vegetative development, the *BTS* RNAi plants were unaffected, whereas at the late reproductive stage, aborted siliques and necrotic lesions in cauline leaves were observed in *BTS* RNAi plants (Supplemental Figures 5C and 5D). Further detailed analysis of Fe distribution verified that the leaves and flowers of *BTS* RNAi plants overaccumulated Fe. Interestingly, the embryo of *BTS* RNAi plants showed obvious Fe staining in the funiculus, indicating excess Fe was imported into the seeds (Supplemental Figures 6A to 6Q). Furthermore, a closer examination of Fe distribution also revealed excess Fe deposition in the phloem of *BTS* RNAi plants (Supplemental Figure 6R).

The findings regarding Fe overaccumulation in *BTS* RNAi and *bts-2* plants were similar to those of *bHLH104* and *ILR3* ox plants, suggesting that BTS may antagonize with them to modulate Fe homeostasis. Thus, we performed a crossing assay and obtained the double mutants of *bhlh104-2* and *bts-2*. When cultivated under Fe-deficient conditions for 2 weeks, the *bhlh104-2 bts-2* lines showed a similar phenotype to the wild type, with shorter roots and more chlorotic leaves compared with *bts-2* (Figure 9A). Interestingly, in the initial stage, the root growth of *bhlh104-2 bts-2* plants was comparable to *bts-2* plants, which was faster than the wild type. However, the root growth of the double mutants was significantly repressed at the beginning of the eighth day, which was also observed in *bhlh104-2* mutants (Figure 9B). This indicates that loss of *bHLH104* could decrease the tolerance of *bts-2* plants to Fe deficiency and the faster growth of *bhlh104-2 bts-2* plants within 1 week might be due to the overaccumulated Fe in their embryos.

Thus, we chose the 8-d-old seedlings grown under Fe-sufficient (+Fe) or Fe-deficient (−Fe+Frz) conditions to test whether the reduced tolerance of *bhlh104-2 bts-2* double mutants relative to *bts-2* plants resulted from impaired transcription of Fe deficiency-responsive genes. Intriguingly, the *bts-2* mutants showed extremely enhanced expression of Ib subgroup *bHLH* genes under Fe-sufficient conditions, and this upregulation was also seen in *bhlh104-2 bts-2* double mutants; however, the degree of elevation was lower than in the *bts-2* mutants (Figure 9C). Under Fe-deficient conditions, levels of these Ib subgroup *bHLH* genes were slightly higher in *bts-2* mutants compared with the wild type, while in the *bhlh104-2 bts-2* double mutants, the expression of *bHLH39* and *bHLH101* was not induced to the same levels as in the wild type; however, they remained higher than in the *bhlh104-2* mutants (Figure 9C). In addition, induction of *PYE*, *ZIF1*, and *NAS4* by Fe deficiency was also lower in the *bhlh104-2 bts-2* double mutants compared with the wild type (Figure 9C). Therefore, loss of *bHLH104* could partially block the activation of Fe deficiency-related genes conferred by *BTS* lesion. Taken together, these genetic studies suggest that bHLH104 may function downstream of BTS to regulate the Fe deficiency responses.

DISCUSSION

It is becoming increasingly clear that a complicated regulatory network is involved in modulating Fe homeostasis. In Arabidopsis, a model requiring two pathways mediated by bHLH family proteins, FIT and PYE, is responsible for the Fe deficiency responses. In this study, we identified two members belonging to the IVc subgroup of bHLH transcription factors, bHLH104 and ILR3, which function as essential regulators in Fe homeostasis.

bHLH104 and ILR3 Are Required to Maintain Fe Homeostasis in Arabidopsis

In Arabidopsis, the large bHLH family contains 162 members, which have been reportedly known to regulate myriad of

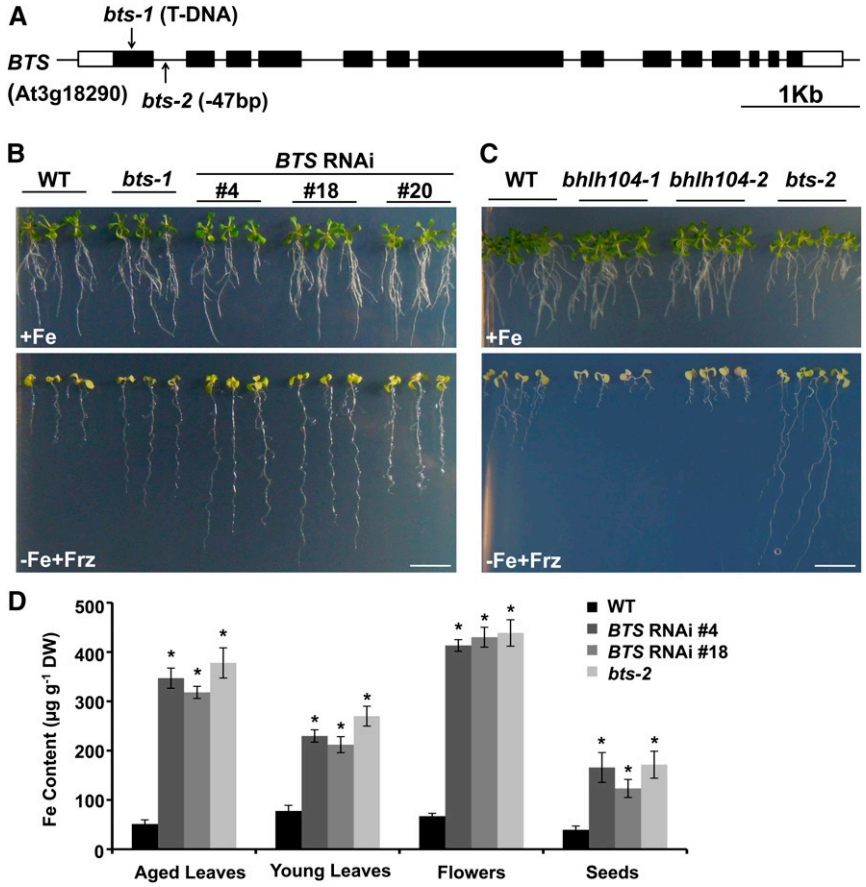

Figure 8. The *BTS* Lesion Plants Display Increased Tolerance to Fe Deficiency.

(A) The position of the T-DNA insertion site for *bts-1* (Salk_016526) mutants and the sequence loss site of *bts-2* mutants.
(B) Phenotypes of wild-type and *BTS* RNAi plants grown for 2 weeks on Fe-sufficient (+Fe) or Fe-deficient (−Fe+Frz) media. Bar = 1 cm.
(C) Phenotypes of wild-type and *bts-2* plants grown for 2 weeks on Fe-sufficient (+Fe) or Fe-deficient (−Fe+Frz) media. Bar = 1 cm.
(D) Fe contents in various tissues of the wild-type, *BTS* RNAi, and *bts-2* plants. Results are means ± SD of three independent experiments. Significant differences from the wild type are indicated by an asterisk ($P < 0.05$), as determined by Student's *t* test.

developmental and physiological responses, one of which is the regulation of Fe deprivation signaling (Bailey et al., 2003; Heim et al., 2003; Li et al., 2006; Pires and Dolan, 2010). In this study, we found that both knockout mutants of *bHLH104* and *ILR3* exhibited severely attenuated responses to Fe deficiency, displaying shorter roots and chlorotic cotyledons (Figures 1C and 5C). By contrast, overexpression of *bHLH104* or *ILR3* in Arabidopsis conferred remarkable tolerance to Fe deficiency (Figures 2 and 6A). Analysis of the expression profiles of known regulatory genes in Fe uptake such as *FIT*, *FRO2*, *IRT1*, and Ib subgroup *bHLH* genes revealed the downregulation of these genes in *bhlh104* and *ilr3* mutants (Table 1, Figure 5E). These results indicate that bHLH104 and ILR3 function positively in the Fe deficiency responses. It is worth mentioning that knockout or overexpression of *bHLH104* and *ILR3* had severe effects on root development in Fe-limited conditions (Figures 1C, 2B, 5C, and 6A), which might have a further effect on Fe absorption. Therefore, the Fe deficiency tolerance and higher Fe contents of *bHLH104* and *ILR3* overexpression plants may be partially ascribed to their large root mass.

Overexpression of *bHLH104* led to excessive Fe accumulation in plants, especially in the phloem (Figure 3P). A similar Fe overload in the phloem was also seen in *nas4x-2*, a nicotianamine loss mutant that cannot remobilize Fe from the phloem to the sink organs, thus resulting in Fe being retained in the phloem and the young leaves being Fe deficient (Klatte et al., 2009; Schuler et al., 2012). However, new leaves of *bHLH104* ox plants did not display an Fe-deficient phenotype, and the expression of *NAS4*, which is involved in nicotianamine biosynthesis, was upregulated in *bHLH104* ox plants (Table 1). This upregulation of *NAS4* could further enhance the transport of Fe from the phloem to mesophyll cells. However, the excessively absorbed Fe is too much to be completely employed, leading to the observed Fe overaccumulation in the phloem of *bHLH104* ox plants.

The transcription factors bHLH104 and ILR3 belong to the IVc subgroup of bHLH family, which has been found widely

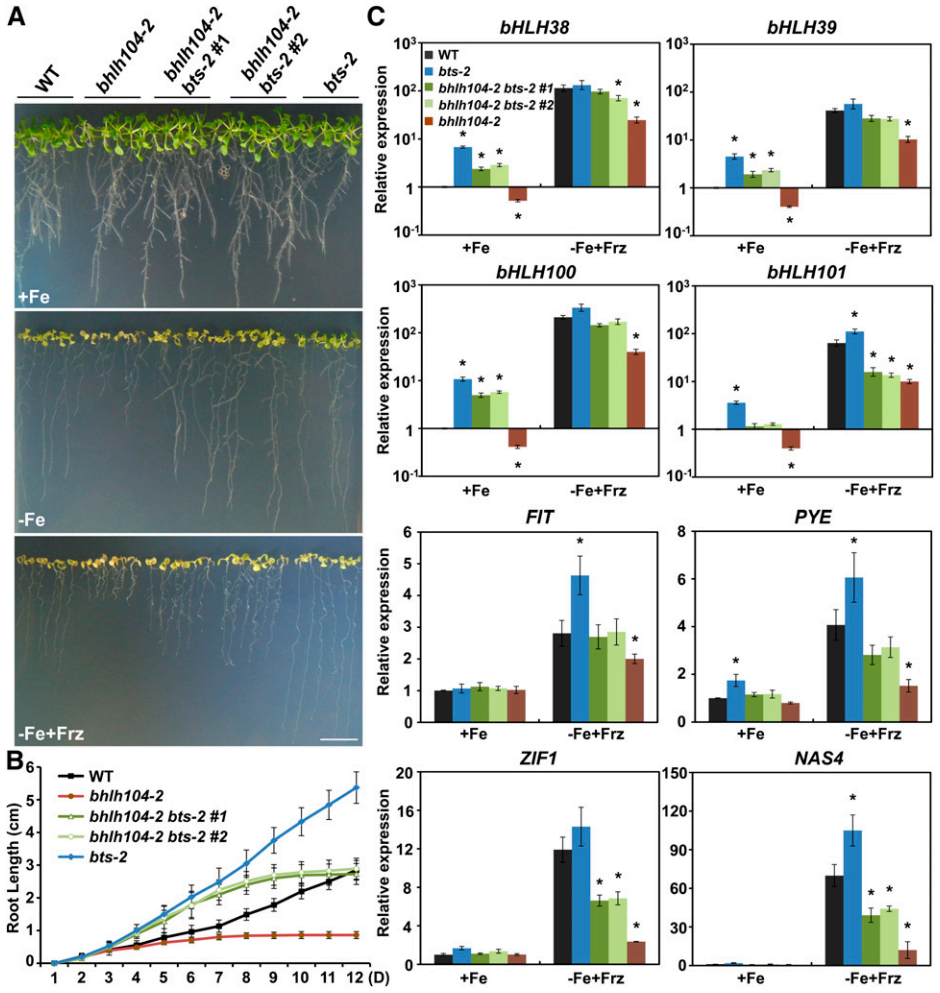

Figure 9. Loss of *bHLH104* Decreases the Tolerance of *bts-2* Plants to Fe Deficiency.

(A) Phenotypes of wild-type and *bhlh104-2 bts-2* plants grown for 2 weeks on Fe-sufficient (+Fe) and Fe-deficient (−Fe and −Fe+Frz) media. Bar = 1 cm.

(B) Quantification of root length of plants on Fe-deficient media (−Fe+Frz) according to the time course. Values are means ± SD of 10 plants for each line.

(C) The relative expression levels of selected Fe deficiency-responsive genes, as measured by qPCR, in roots of the wild type, *bts-2* mutants, and *bhlh104-2 bts-2* double mutants grown on Fe-sufficient (+Fe) or Fe-deficient (−Fe+Frz) media for 8 d. The expression of *TUB2* was used to normalize mRNA levels, and the gene expression levels in the wild type under Fe-sufficient conditions were set to 1. The data represent means ± SD of three independent experiments. Significant differences from the corresponding wild type are indicated by an asterisk ($P < 0.05$), as determined by Student's *t* test.

conserved in flowering plants, such as rice, tomato, soybean (*Glycine max*), and grape (*Vitis vinifera*; Pires and Dolan, 2010). Analysis of miRNA macroarrays predicted that *Phaseolus vulgaris* miR1509 might target *bHLH104* during the Mn stress response (Valdés-López et al., 2010; Gupta et al., 2014). Moreover, the *Chlamydomonas reinhardtii* bHLH protein Cre24.g770450, which is similar to the Arabidopsis subgroup IVc transcription factors, is induced in Fe-poor conditions (Urzica et al., 2012). Recently, a bHLH transcription factor in chrysanthemum (*Chrysanthemum* × *morifolium*), Cm-bHLH1, which is highly similar to ILR3, was shown to regulate Fe intake under Fe deficiency (Zhao et al., 2014). These findings hint that the IVc subgroup bHLH transcription factors may have conserved functions in plant metal homeostasis.

Both bHLH104 and ILR3 Regulate the Promoters of Ib Subgroup *bHLH* Genes

The bHLH domain comprises two regions. The C-terminal HLH region is responsible for forming homo- or heterodimers, while the N-terminal basic region determines the DNA-protein interaction by binding to canonical E-box (G-box) or noncanonical E-box motifs (Toledo-Ortiz et al., 2003; Li et al., 2006). For example,

CRYPTOCHROME-INTERACTING bHLH1 (CIB1) can form heterodimers with CIB2, CIB4, and CIB5 and bind to the noncanonical E-box sequence of the *FT* promoter in vivo (Liu et al., 2013). The Arabidopsis tapetum development regulator DYSFUNCTIONAL TAPETUM1 forms homodimers and also interacts with three other bHLH proteins, bHLH10, bHLH89, and bHLH91 (Feng et al., 2012). These results indicate that dimerization of bHLH proteins is important for specifically binding the promoters of target genes.

Here, we demonstrated that bHLH104 could interact with ILR3 and both of them bound to the canonical E-box of *bHLH38*, *bHLH100*, *bHLH101*, and *PYE* with much higher affinity than with noncanonical E-box DNA sequences. In addition, they also associated with the chromatin region of the *bHLH39* promoter, which only contains noncanonical E-box sequences (Figure 7). In previous studies, these Ib subgroup *bHLH* genes were demonstrated to be widely expressed in various tissues, especially in the epidermis of roots and veins of leaves (Wang et al., 2007). Similarly, *bHLH104* is ubiquitously expressed in both roots and leaves. In particular, it is highly expressed in the root stele and leaf vasculature (Supplemental Figure 7). This tissue expression pattern was also observed for *ILR3* using β-glucuronidase (GUS) activity analysis of its promoter (Rampey et al., 2006). Furthermore, the induction of four Ib subgroup *bHLH* genes was extremely repressed upon Fe deficiency in the absence of bHLH104 or ILR3 (Table 1, Figure 5E). Therefore, we conclude that bHLH104 and ILR3 are the direct upstream activators of Ib subgroup *bHLH* genes. Although the upregulation of *FIT* under Fe deficiency was also inhibited in both *bhlh104* and *ilr3* mutants (Table 1, Figure 5E), there was no detectable binding to the *FIT* promoter by bHLH104 or ILR3. This suggested the existence of other intermediate transcription factors that act upon *FIT* but are downstream regulators of bHLH104 and ILR3. bHLH104 could also interact with bHLH115 and a slight interaction was seen between bHLH104 and bHLH34 (Figure 4), suggesting putative roles of bHLH115 and bHLH34 in Fe homeostasis regulation. Moreover, this also implies that bHLH104 may dimerize with more than one partner to specifically regulate target genes.

Although bHLH104 and ILR3 could form heterodimers, and both of them targeted Ib subgroup *bHLH* gene promoters, the BiFC assay also suggested that bHLH104 and ILR3 could interact with themselves (Figure 4A). Furthermore, the overexpression of bHLH104 and ILR3 exhibited more tolerance to Fe deficiency stress and resulted in Fe overload (Figures 2 and 6). This is quite different from FIT. Despite the fact that FIT could form homodimers, overexpression of *FIT* alone did not lead to any obvious phenotype or detectable change of Fe contents in shoots, since FIT must interact with a Ib subgroup bHLH protein to drive the expression of *FRO2* and *IRT1* (Yuan et al., 2008). These findings indicated that bHLH104 and ILR3 could both promote Fe accumulation without necessarily relying on each other. Comparison of the physiological response to Fe deficiency revealed that *ilr3* mutants appeared more sensitive than *bhlh104*, since the *bhlh104* mutants could develop true leaves, while the *ilr3* mutants were stunted with only two pieces of chlorotic cotyledons (Figure 5C). Moreover, the overexpression of *ILR3* resulted in chlorotic leaves that were not seen in *bHLH104* ox plants (Figure 6B), suggesting that they might act independently on different downstream targets. Thus, the response to Fe deficiency requires the activities of both bHLH104 and ILR3.

BTS and bHLH104 Probably Function in the Same Pathway in Fe Homeostasis

To date, several candidates for a long-distance Fe signal have been characterized in Arabidopsis; however, the mechanisms of sensing cellular Fe status remain unclear (Walker and Connolly, 2008; Hindt and Guerinot, 2012). In Arabidopsis, BTS is a homolog of HRZs and FBXL5, the known Fe sensors in rice and mammals, which negatively regulate Fe acquisition (Salahudeen et al., 2009; Vashisht et al., 2009). In a previous study, a partial loss-of-function allele of *BTS*, *bts-1*, was reported to confer tolerance to Fe deficiency (Long et al., 2010); however, the Fe content and gene expression regulation still remain unclear. Here, we showed that plants with a lesion in *BTS* were capable to accumulate excess Fe and the expression of Fe deficiency-inducible genes was substantially enhanced (Figures 8D and 9C). These characteristics are very similar to those of the rice HRZs knockdown plants (Kobayashi et al., 2013), confirming their conserved functions of negatively regulating Fe uptake in plants. Furthermore, HRZ1/2 and BTS can all bind Fe and Zn and have E3 ligase activity (Kobayashi et al., 2013). Thus, BTS may function as a Fe sensor in Arabidopsis by regulating the stability of downstream factors.

Loss of *bHLH104* could decrease the tolerance to Fe deficiency conferred by *BTS* lesion, which suggested an opposite function between BTS and bHLH104 in Fe homeostasis. Both of them are located in the nucleus and have been found to interact with each other in a yeast two-hybrid assay (Long et al., 2010; Kobayashi et al., 2013). Moreover, genes responding to Fe deficiency that

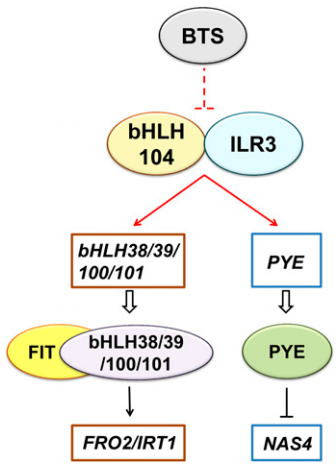

Figure 10. Model of bHLH104- and ILR3-Mediated Fe Deficiency Responses.

The model depicts the molecular function of bHLH104 and ILR3 in Arabidopsis Fe homeostasis relative to other known bHLH regulators. bHLH104 interacts with ILR3 and both of them regulate the expression of Ib subgroup *bHLH* genes and *PYE* by binding to their promoters. bHLH104 and ILR3 might be the downstream targets of an E3 ubiquitin ligase, BTS, which negatively regulates Fe absorption and was previously found to interact with bHLH104 and ILR3. The data generated in this study are indicated by red lines, while those from previous studies are indicated by black lines. Ovals represent central regulatory proteins and squares represent the downstream target genes.

were downregulated in *bhlh104* mutants were upregulated in *BTS* RNAi lines (Table 1, Figure 9C). These traits indicate that bHLH104 and BTS might work in a common pathway to regulate Fe homeostasis. In Arabidopsis, several E3 ligases have been reported to regulate the abundance of transcription factors. For example, the RING-type E3 ligase, KEEP ON GOING, is a negative regulator of abscisic acid and ubiquitinates the transcription factor ABSCISIC ACID INSENSITIVE5 following abscisic acid treatment (Liu and Stone, 2010). Hence, BTS might control Fe contents in plants by regulating the abundance of bHLH104 and ILR3. Recently, a study by Selote et al. (2015) demonstrated that BTS could target ILR3 and bHLH115 but not bHLH104 for the 26S proteasome-mediated degradation, using a cell-free degradation assay. However, the mutation of bHLH104 could partially complement the phenotype of *BTS* lesion (Figure 9), which suggested that the loss of *bHLH104* might disrupt the formation of heterodimers with ILR3 and bHLH115 that function to activate the Fe deficiency responses in *bts-2* plants. In future studies, a triple or tetra mutant should be constructed to further clarify the regulatory mechanism between BTS and these IVc subgroup bHLH proteins.

This regulatory network involving BTS-bHLH104/ILR3-Ib subgroup bHLH transcription factors/PYE in Arabidopsis raised the question of whether this regulatory mechanism also exists in Strategy II plants, since the Fe deficiency response has been demonstrated to be partially conserved between graminaceous and nongraminaceous plants (Kobayashi and Nishizawa, 2012). To date, the downstream regulator of rice HRZs has not been identified. However, knockdown of HRZs resulted in the upregulation of rice IRO2 and IRO3, which are the orthologs of Arabidopsis bHLH38/39 and PYE, respectively (Ogo et al., 2006; Zheng et al., 2010; Kobayashi et al., 2013). bHLH38/39 and PYE are both downstream regulators of bHLH104 and ILR3; therefore, we wondered whether there also exist transcription factors acting upstream of IRO2 and IRO3 in rice, which play a similar role to bHLH104 and ILR3. Interestingly, the core sequence for rice *IRO2* promoter binding was determined to be CACGTGG in a biochemical analysis (Ogo et al., 2006), implying that the transcriptional activation of *IRO2* may also be via bHLH-associated E-box elements in its promoter. Thus, further study on the regulatory network of Strategy II plants would be of interest.

In summary, our results provide evidence that the IVc subgroup bHLH transcription factors bHLH104 and ILR3 act as positive regulators in the Fe deficiency responses. bHLH104 and ILR3 could form heterodimers, and both of them bind to the promoters of subgroup Ib *bHLH* genes and *PYE*, functioning as upstream regulators of these two transcriptional regulation pathways. We also demonstrate that bHLH104 acts downstream of BTS, which negatively regulate Fe uptake in Arabidopsis (Figure 10). This regulatory network provides insight into the mechanism of plants' responses to Fe deficiency and also offers a strategy for the design and breeding of Fe-deficient crops by genetic manipulation of regulatory genes. However, it is important to ensure reasonable Fe absorption, since excess Fe can cause a decrease in fertility. Future investigations of other two transcription factors belonging to the IVc subgroup will be meaningful, and clarification of the relationship between BTS and the IVc subgroup bHLH transcription factors would be of great interest.

METHODS

Plant Materials and Growth Conditions

The *Arabidopsis thaliana* ecotype Columbia-0 was used as the wild type in this study. The T-DNA insertion lines for *bhlh104-1* (Salk_099496C), *bhlh104-2* (Salk_043862C), *ilr3-2* (Salk_004997C), and *ilr3-3* (Salk_043690C) were confirmed using PCR with a T-DNA primer (*Lba*I) and gene-specific primers (Supplemental Table 1). The *bhlh104-2 bts-2* double mutant plants were generated by crossing *bhlh104-2* as the female parent, to *bts-2* mutants; and two double mutant lines were studied in this work, named *bhlh104-2 bts-2* #1 and *bhlh104-2 bts-2* #2. For normal soil cultivation, plants were grown under light at 120 μM photons m^{-2} s^{-1}, a 16-h/8-h light/dark cycle, 23°C /19°C day/night, and relative air humidity of 50 to 70%. High-pH soil (pH 7 to 8) was generated by adding CaO to soil, as described previously (Kim et al., 2006).

For phenotypic analyses of the Fe deprivation response, seeds were surface sterilized using 70% ethanol for 1 min followed by 20% bleach for 20 min and sown on Fe-sufficient media [+Fe, half Murashige and Skoog (MS) media containing 100 μM Fe(II)-EDTA with 1% sucrose and 1% agar] or Fe-deficient media [−Fe, without Fe(II)-EDTA; −Fe+Frz, with 50 μM ferrous chelate ferrozine]. After vernalization in darkness at 4°C for 3 d, the plates were placed in light with an irradiance of 120 μM photons m^{-2} s^{-1} for the indicated days at 23°C/19°C day/night.

Plasmid Construction and Plant Transformation

To construct the plants overexpressing *bHLH104* or *ILR3*, the coding sequences of *bHLH104* and *ILR3* and a C-terminal GFP fusion sequence were amplified with gene-specific primers (Supplemental Table 1). The open reading frame was cloned into pRi35S and then cleaved by *Stu*I/*Kpn*I and inserted into pCAMBIA1301 to generate *35S:bHLH104-GFP* and *35S:ILR3-GFP* constructs. To produce *BTS*-silenced plants, 1000-bp sense and antisense sequences of *BTS* were cloned into pRi35S and then inserted into pCAMBIA1301. The different constructs were introduced into *Agrobacterium tumefaciens* strain EHA105 by heat shock. The transformants were then transformed into Columbia-0 plants through the floral dipping method (Clough and Bent, 1998). Transgenic plants were selected on half-strength MS agar plates with hygromycin, and homozygous T3 lines were used for subsequent analyses.

Rhizosphere Acidification, Ferric-Chelate Reductase Assays, and Tissue Elemental Analyses

The rhizosphere acidification assays were conducted as previously described (Yi and Guerinot, 1996). Seeds were germinated on Fe-sufficient or Fe-deficient media for 7 d, and four plants of every line were transferred to 1% agar plates containing 0.006% bromocresol purple and 0.2 mM $CaSO_4$ (pH adjusted to 6.5 with NaOH) for 24 h.

Root ferric-chelate reductase activity was measured spectrophotometrically as described previously (Lucena et al., 2006). Ten intact plants of every line were pretreated for 30 min in plastic vessels with 4 mL half-strength MS solution without micronutrients (pH 5.5) and then soaked into 4 mL Fe(III) reduction assay solution [half-strength MS without micronutrients, 100 μM Fe(III)-EDTA, and 300 μM ferrozine, pH adjusted to 5.0 with KOH] for 30 min in darkness. An identical assay solution containing no plants was used as a blank. The purple-colored Fe(II)-ferrozine complex was quantified at 562 nm using a molar extinction coefficient of 28.6 mM^{-1} cm^{-1}.

For tissue elemental analyses, seeds were placed on the Fe-sufficient or Fe-deficient media in a single row at a density of ~15 seeds/cm for 8 d. Shoots of seedlings of four plates were collected to generate at least 200 mg of fresh weight. Tissue samples were dried at 80°C for 24 h to yield ~20 to 40 mg tissue for elemental analyses. After cooling, all samples were digested with 10 mL concentrated nitric acid/perchloric acid (3:1) and diluted to 10 mL

in 18 Ω water. The Fe contents were analyzed by inductively coupled plasma-atomic emission spectrometry, as described previously (Herbik et al., 2002).

Perls Staining for Fe, Tissue Sectioning, and DAB/H_2O_2 Intensification

For Fe^{3+} localization, plant tissues were vacuum infiltrated with Perls stain solution (equal volumes of 4% [v/v] HCl and 4% [w/v] K-ferrocyanide) for 30 min. Then the plant samples were incubated for another 1 h in the stain solution and rinsed three times with distilled water. For leaf staining, plant tissues were first incubated with fixative solution (methanol/chloroform/acetic acid, 6:3:1) for 1 h at room temperature and then added to the Perls stain solution. Localization of Fe^{3+} was observed using a stereomicroscope (SteREO Lumar.V12).

For tissue sectioning, leaves from adult plants were obtained at bolting and were fixed overnight at 4°C in FAA fixing buffer (containing 2% formaldehyde, 50% ethanol, and 5% acetic acid). Fixed tissues were dehydrated in 10, 30, 50, 60, 70, 80, 90, and 100% ethanol for 1 h at each concentration and then embedded in paraffin (Leica). Transverse sections (4 μm) were obtained using a Leica RM 2145 microtome.

The DAB intensification reaction was performed as previously described (Meguro et al., 2007; Roschzttardtz et al., 2009). The paraffin sections were dewaxed and rehydrated, placed into Perls stain solution for 30 min, and subsequently washed with distilled water. The sections were then incubated in a methanol solution containing 0.01 M NaN_3 and 0.3% (v/v) H_2O_2 for 1 h and washed with 0.1 M phosphate buffer (pH 7.4). Then the sections were incubated in an intensification solution (0.1 M phosphate buffer solution containing 0.025% [w/v] DAB, 0.005% [v/v] H_2O_2, and 0.005% [w/v] $CoCl_2$, pH 7.4) for 20 min and washed with distilled water to stop the reaction.

Total Chlorophyll Content Analyses

Total chlorophyll was extracted from leaves with 80% acetone in 2.5 mM HEPES-KOH (pH 7.5), and the chlorophyll content was determined as previously described (Wellburn, 1994).

RT-PCR and qPCR

To test for full-length *bHLH104* transcript in the wild type and the *bhlh104* mutants, leaves of plants grown for 4 weeks in normal soil were collected. Total RNA was extracted using a Plant RNA Kit (Omega) and 5 μg total RNA was used for cDNA synthesis using the PrimeScript RT reagent kit (Takara). The amplification of full-length *bHLH104* transcript was performed using gene-specific primers (Supplemental Table 1), and *UBQ10* was used as a control gene. PCR amplifications were done for 28 and 25 cycles for *bHLH104* and *UBQ10*, respectively. For qPCR analyses, roots of seedlings grown on Fe-sufficient or Fe-deficient media were collected respectively to generate ~50 mg fresh weight for RNA extraction. qPCR was performed using SYBR Premix Ex Taq (Takara), and amplification was monitored in real-time on the LightCycler 480 (Roche). *TUBULIN2* (*TUB2*) was amplified as an internal control, and gene copy number was normalized to that of *TUB2*. *TUB2* was relatively stable during different Fe supply when compared with the relative gene expression of *ACTIN2* and *UBQ4*; thus, *TUB2* was used as an internal control in this study. The primers used for qPCR analyses are listed in Supplemental Table 1.

Protein Extraction and Immunoblotting

To analyze the protein expression in transgenic plants, total proteins were extracted with protein extraction buffer (50 mM Tris-HCl at pH 7.5, 150 mM NaCl, 5 mM EDTA, 0.1% Triton X-100, and protease inhibitor cocktail [Roche]). The extracts were subsequently centrifuged at 18,000*g* for 10 min at 4°C to collect the supernatants for immunoblot analyses. Total proteins (200 μg) were separated by SDS-PAGE. After electrophoresis, the proteins were transferred to polyvinylidene difluoride membranes (Millipore) and probed using antibodies specifically directed against GFP (Abmart).

Arabidopsis Protoplast Preparation and Transfection

The protoplast isolation from Arabidopsis leaves was performed as previously described (Zhai et al., 2009). Briefly, 14-d-old Arabidopsis leaves were cut into strips in TVL solution (0.3 M sorbitol and 50 mM $CaCl_2$) and then incubated in enzyme solution (0.5 M sucrose, 10 mM MES-KOH at pH 5.7, 20 mM $CaCl_2$, 40 mM KCl, 1% Cellulase R-10, and 1% Macerozyme R-10) with gentle shaking for 16 h in the dark. The protoplasts were collected by centrifugation at 100*g* for 7 min and washed twice with W5 solution (0.1% glucose, 0.08% KCl, 0.9% NaCl, 1.84% $CaCl_2$, and 2 mM MES at pH 5.7). For BiFC analyses, 10 μg plasmid DNA per 100 μL (~5×10^4 cells) Arabidopsis protoplasts was used for transfection. As a positive control, both bZIP63 fused with YN and bZIP63 fused with YC were cotransfected into protoplasts. After incubation for 12 h, the protoplasts were harvested and fluorescence emission of YFP in protoplasts was observed under a confocal microscope (TCS-SP5; Leica) as previously described (Yuan et al., 2008).

GST Pull-Down and Co-IP Assays

For pull-down assays, 4 mL Arabidopsis protoplasts (~2×10^6 cells) was transfected with 400 μg *35S:ILR3-GFP* or *35S:bHLH115-GFP* plasmids and cultured in the dark for 16 h. The protoplasts were then harvested by centrifugation at 100*g* for 7 min. Total proteins were extracted with 1 mL protein extraction buffer. A portion of the protein extracts (500 μL) was mixed with 50 μg purified recombinant GST-bHLH104 and the remaining extract was mixed with 50 μg GST as a negative control. Then, 30 μL glutathione Sepharose 4B (GE Healthcare) was added to the samples. After incubation for 6 h with constant rotation at 4°C, the Sepharose was washed five times with ice-cold PBS buffer (pH 7.4), and bound proteins were eluted with 30 μL elution buffer (30 mM glutathione in PBS buffer). For immunoblotting analyses, 20 μL protein extract before incubation was used as input and 30 μL eluate was loaded as the immunoprecipitate.

For co-IP assays, 4 mL Arabidopsis protoplasts was cotransfected with 400 μg *35S:bHLH104-Flag* and 400 μg *35S:ILR3-GFP* or 400 μg *35S:ILR3-GFP* alone (same for *35S:bHLH115-GFP*). Total proteins were extracted with 500 μL protein extraction buffer and 20 μL protein extract was used as input. The total cell extracts were further incubated with 30 μL anti-FLAG M2 affinity gel (Sigma-Aldrich) for 6 h at 4°C with rotation. After washing five times with ice-cold TBS buffer (pH 7.4), the bound proteins were eluted by boiling the gel using 30 μL SDS-PAGE sample buffer without β-mercaptoethanol and loaded onto SDS-PAGE for immunoblotting.

ChIP

ChIP was performed following a previously described protocol (Saleh et al., 2008), using 10 mL Arabidopsis protoplasts transfected with 1 mg *35S:bHLH104-Flag* or *35S:ILR3-Flag* plasmids. Ten milliliters of protoplasts without transfection was used as a negative control. After transfection for 24 h, the protoplasts were fixed with 1% formaldehyde for 15 min and neutralized with 0.125 M glycine for 5 min. After washing twice with W5 solution, the protoplasts were harvested by centrifugation at 100*g* for 3 min and suspended in SDS lysis buffer (50 mM Tris-HCl at pH 7.5, 150 mM NaCl, 1 mM PMSF, 1 mM EDTA, 1% SDS, 1% Triton X-100, and 0.1% sodium deoxycholate) for sonication. Then, 50 μL anti-FLAG M2 affinity gel (Sigma-Aldrich) was used for each immunoprecipitation and the enriched DNA fragments were analyzed by qPCR using the primers listed in Supplemental Table 2. The amount of ChIP-DNA coprecipitated by anti-FLAG M2 affinity gel was first normalized by comparing to the total input DNA used for each

immunoprecipitation $C_T = C_T(\text{ChIP}) - C_T(\text{input})$. Then, these normalized ChIP signals were compared between the detecting targets and the E-box motif of *TUB2*, which was used as a negative control. The binding of *TUB2* promoter in the protoplast without transfection was set to 1, and the DNA binding ratio was given as the fold increase in signal relative to *TUB2*'s binding. A 3-fold DNA binding ratio relative to *TUB2*'s binding was used as the threshold in this study.

Histochemical GUS Staining Assays

To investigate the *bHLH104* expression pattern, the 1474-bp sequence upstream of the ATG codon in the *bHLH104* gene was amplified with specific primers (Supplemental Table 1). The promoter was cloned into pCAMBIA1381 to drive the expression of the GUS reporter gene. For the GUS staining, tissues were soaked overnight in GUS-staining buffer as previous described (Jefferson et al., 1987) and then washed with 70% ethanol. Images were captured under a stereomicroscope.

Accession Numbers

Sequence data from this article can be found in the GenBank/EMBL data libraries under the following accession numbers: *bHLH104* (At4g14410), *ILR3* (At5g54680), *bHLH34* (At3g23210), *bHLH115* (At1g51070), *bHLH38* (At3g56970), *bHLH39* (At3g56980), *bHLH100* (At2g41240), *bHLH101* (At5g04150), *PYE* (At3g47640), *BTS* (At3g18290), *FIT* (At2g28160), *FRO2* (At1g01580), *IRT1* (At4g19690), *IRT2* (At4g19680), *FER1* (At5g01600), *YSL1* (At4g24120), *NAS4* (At1g56430), *ZIF1* (At5g13740), *FRD3* (At3g08040), *MYB10* (At3g12820), *MYB72* (At1g56160), *UBQ10* (At4g05320), and *TUB2* (At5g62690).

Supplemental Data

Supplemental Figure 1. Phenotypic analyses of the wild type, *bhlh104-1*, and *bhlh104-2* in response to Fe deficiency.

Supplemental Figure 2. Phenotypic analyses of wild-type and *bhlh104-2* complemented plants in response to Fe deficiency.

Supplemental Figure 3. Quantification of root length of *bHLH104* ox plants and Trypan blue staining of necrosis in *bHLH104* ox leaves.

Supplemental Figure 4. Identification of *ILR3* ox plants and Trypan blue staining of necrosis in *ILR3* ox leaves.

Supplemental Figure 5. Plants silenced with *BTS* exhibit reduced fertility.

Supplemental Figure 6. Perls staining for Fe^{3+} of *BTS* RNAi plants.

Supplemental Figure 7. Expression pattern analysis of *bHLH104*.

Supplemental Table 1. Primers used to identify T-DNA insertion mutants, gene cloning, and qPCR.

Supplemental Table 2. Primers used for ChIP-qPCR.

Supplemental Methods. Trypan blue staining.

ACKNOWLEDGMENTS

We thank Philip N. Benfey (University of Illinois at Chicago) for kindly sending us the *bts-1* mutant seeds. We appreciate the gift of *ilr3-2* seeds from Bonnie Bartel (Rice University at Houston). We thank Terri A. Long (North Carolina State University) for kindly providing experimental guidance. We also thank the ABRC for the seed stocks. This investigation was supported by the National Natural Science Foundation of China (No. 31370297 and No. 31425003), the Natural Science Foundation of Guangdong Province, PR China (No. S2013010012682), and the Fundamental Research Funds for the Central Universities.

AUTHOR CONTRIBUTIONS

H.-B.W. and J.Z. designed the study. J.Z. and M.L. performed research. J.Z., B.L., D.F., and J.W. analyzed data. J.Z. and H.-B.W. wrote the article. B.L., H.J., P.W., J.L., and F.X. revised the article.

Received October 14, 2014; revised February 2, 2015; accepted February 17, 2015; published March 20, 2015.

REFERENCES

Bailey, P.C., Martin, C., Toledo-Ortiz, G., Quail, P.H., Huq, E., Heim, M.A., Jakoby, M., Werber, M., and Weisshaar, B. (2003). Update on the basic helix-loop-helix transcription factor gene family in Arabidopsis thaliana. Plant Cell **15:** 2497–2502.

Bauer, P., Ling, H.Q., and Guerinot, M.L. (2007). FIT, the FER-LIKE IRON DEFICIENCY INDUCED TRANSCRIPTION FACTOR in Arabidopsis. Plant Physiol. Biochem. **45:** 260–261.

Clough, S.J., and Bent, A.F. (1998). Floral dip: a simplified method for Agrobacterium-mediated transformation of *Arabidopsis thaliana*. Plant J. **16:** 735–743.

Colangelo, E.P., and Guerinot, M.L. (2004). The essential basic helix-loop-helix protein FIT1 is required for the iron deficiency response. Plant Cell **16:** 3400–3412.

Curie, C., and Briat, J.F. (2003). Iron transport and signaling in plants. Annu. Rev. Plant Biol. **54:** 183–206.

Fan, H., Zhang, Z., Wang, N., Cui, Y., Sun, H., Liu, Y., Wu, H., Zheng, S., Bao, S., and Ling, H.Q. (2014). SKB1/PRMT5-mediated histone H4R3 dimethylation of Ib subgroup bHLH genes negatively regulates iron homeostasis in *Arabidopsis thaliana*. Plant J. **77:** 209–221.

Feng, B., Lu, D., Ma, X., Peng, Y., Sun, Y., Ning, G., and Ma, H. (2012). Regulation of the Arabidopsis anther transcriptome by DYT1 for pollen development. Plant J. **72:** 612–624.

Fisher, F., and Goding, C.R. (1992). Single amino acid substitutions alter helix-loop-helix protein specificity for bases flanking the core CANNTG motif. EMBO J. **11:** 4103–4109.

Fox, T.C., and Guerinot, M.L. (1998). Molecular biology of cation transport in plants. Annu. Rev. Plant Physiol. Plant Mol. Biol. **49:** 669–696.

Green, L.S., and Rogers, E.E. (2004). FRD3 controls iron localization in Arabidopsis. Plant Physiol. **136:** 2523–2531.

Grusak, M.A., Welch, R.M., and Kochian, L.V. (1990). Physiological characterization of a single-gene mutant of *Pisum sativum* exhibiting excess iron accumulation: I. Root iron reduction and iron uptake. Plant Physiol. **93:** 976–981.

Guerinot, M.L., and Yi, Y. (1994). Iron: nutritious, noxious, and not readily available. Plant Physiol. **104:** 815–820.

Gupta, O.P., Sharma, P., Gupta, R.K., and Sharma, I. (2014). MicroRNA mediated regulation of metal toxicity in plants: present status and future perspectives. Plant Mol. Biol. **84:** 1–18.

Hänsch, R., and Mendel, R.R. (2009). Physiological functions of mineral micronutrients (Cu, Zn, Mn, Fe, Ni, Mo, B, Cl). Curr. Opin. Plant Biol. **12:** 259–266.

Haydon, M.J., and Cobbett, C.S. (2007). A novel major facilitator superfamily protein at the tonoplast influences zinc tolerance and accumulation in Arabidopsis. Plant Physiol. **143:** 1705–1719.

Heim, M.A., Jakoby, M., Werber, M., Martin, C., Weisshaar, B., and Bailey, P.C. (2003). The basic helix-loop-helix transcription factor family in plants: a genome-wide study of protein structure and functional diversity. Mol. Biol. Evol. **20:** 735–747.

Hell, R., and Stephan, U.W. (2003). Iron uptake, trafficking and homeostasis in plants. Planta **216:** 541–551.

Herbik, A., Bölling, C., and Buckhout, T.J. (2002). The involvement of a multicopper oxidase in iron uptake by the green algae *Chlamydomonas reinhardtii*. Plant Physiol. **130:** 2039–2048.

Hindt, M.N., and Guerinot, M.L. (2012). Getting a sense for signals: regulation of the plant iron deficiency response. Biochim. Biophys. Acta **1823:** 1521–1530.

Ivanov, R., Brumbarova, T., and Bauer, P. (2012). Fitting into the harsh reality: regulation of iron-deficiency responses in dicotyledonous plants. Mol. Plant **5:** 27–42.

Jefferson, R.A., Kavanagh, T.A., and Bevan, M.W. (1987). GUS fusions: beta-glucuronidase as a sensitive and versatile gene fusion marker in higher plants. EMBO J. **6:** 3901–3907.

Kim, S.A., Punshon, T., Lanzirotti, A., Li, L., Alonso, J.M., Ecker, J.R., Kaplan, J., and Guerinot, M.L. (2006). Localization of iron in Arabidopsis seed requires the vacuolar membrane transporter VIT1. Science **314:** 1295–1298.

Klatte, M., Schuler, M., Wirtz, M., Fink-Straube, C., Hell, R., and Bauer, P. (2009). The analysis of Arabidopsis nicotianamine synthase mutants reveals functions for nicotianamine in seed iron loading and iron deficiency responses. Plant Physiol. **150:** 257–271.

Kneen, B.E., Larue, T.A., Welch, R.M., and Weeden, N.F. (1990). Pleiotropic effects of brz: A mutation in *Pisum sativum* (L.) cv; Sparkle' conditioning decreased nodulation and increased iron uptake and leaf necrosis. Plant Physiol. **93:** 717–722.

Kobayashi, T., and Nishizawa, N.K. (2012). Iron uptake, translocation, and regulation in higher plants. Annu. Rev. Plant Biol. **63:** 131–152.

Kobayashi, T., Nakanishi, H., and Nishizawa, N.K. (2010). Recent insights into iron homeostasis and their application in graminaceous crops. Proc. Jpn. Acad. Ser. B Phys. Biol. Sci. **86:** 900–913.

Kobayashi, T., Nagasaka, S., Senoura, T., Itai, R.N., Nakanishi, H., and Nishizawa, N.K. (2013). Iron-binding haemerythrin RING ubiquitin ligases regulate plant iron responses and accumulation. Nat. Commun. **4:** 2792.

Li, X., et al. (2006). Genome-wide analysis of basic/helix-loop-helix transcription factor family in rice and Arabidopsis. Plant Physiol. **141:** 1167–1184.

Ling, H.Q., Bauer, P., Bereczky, Z., Keller, B., and Ganal, M. (2002). The tomato fer gene encoding a bHLH protein controls iron-uptake responses in roots. Proc. Natl. Acad. Sci. USA **99:** 13938–13943.

Liu, H., and Stone, S.L. (2010). Abscisic acid increases Arabidopsis ABI5 transcription factor levels by promoting KEG E3 ligase self-ubiquitination and proteasomal degradation. Plant Cell **22:** 2630–2641.

Liu, Y., Li, X., Li, K., Liu, H., and Lin, C. (2013). Multiple bHLH proteins form heterodimers to mediate CRY2-dependent regulation of flowering-time in Arabidopsis. PLoS Genet. **9:** e1003861.

Long, T.A., Tsukagoshi, H., Busch, W., Lahner, B., Salt, D.E., and Benfey, P.N. (2010). The bHLH transcription factor POPEYE regulates response to iron deficiency in Arabidopsis roots. Plant Cell **22:** 2219–2236.

Lucena, C., Waters, B.M., Romera, F.J., García, M.J., Morales, M., Alcántara, E., and Pérez-Vicente, R. (2006). Ethylene could influence ferric reductase, iron transporter, and H+-ATPase gene expression by affecting FER (or FER-like) gene activity. J. Exp. Bot. **57:** 4145–4154.

Meguro, R., Asano, Y., Odagiri, S., Li, C., Iwatsuki, H., and Shoumura, K. (2007). Nonheme-iron histochemistry for light and electron microscopy: a historical, theoretical and technical review. Arch. Histol. Cytol. **70:** 1–19.

Mendoza-Cózatl, D.G., Xie, Q., Akmakjian, G.Z., Jobe, T.O., Patel, A., Stacey, M.G., Song, L., Demoin, D.W., Jurisson, S.S., Stacey, G., and Schroeder, J.I. (2014). OPT3 is a component of the iron-signaling network between leaves and roots and misregulation of OPT3 leads to an over-accumulation of cadmium in seeds. Mol. Plant **7:** 1455–1469.

Ogo, Y., Itai, R.N., Kobayashi, T., Aung, M.S., Nakanishi, H., and Nishizawa, N.K. (2011). OsIRO2 is responsible for iron utilization in rice and improves growth and yield in calcareous soil. Plant Mol. Biol. **75:** 593–605.

Ogo, Y., Itai, R.N., Nakanishi, H., Kobayashi, T., Takahashi, M., Mori, S., and Nishizawa, N.K. (2007). The rice bHLH protein OsIRO2 is an essential regulator of the genes involved in Fe uptake under Fe-deficient conditions. Plant J. **51:** 366–377.

Ogo, Y., Itai, R.N., Nakanishi, H., Inoue, H., Kobayashi, T., Suzuki, M., Takahashi, M., Mori, S., and Nishizawa, N.K. (2006). Isolation and characterization of IRO2, a novel iron-regulated bHLH transcription factor in graminaceous plants. J. Exp. Bot. **57:** 2867–2878.

Pires, N., and Dolan, L. (2010). Origin and diversification of basic-helix-loop-helix proteins in plants. Mol. Biol. Evol. **27:** 862–874.

Rampey, R.A., Woodward, A.W., Hobbs, B.N., Tierney, M.P., Lahner, B., Salt, D.E., and Bartel, B. (2006). An Arabidopsis basic helix-loop-helix leucine zipper protein modulates metal homeostasis and auxin conjugate responsiveness. Genetics **174:** 1841–1857.

Ravet, K., Touraine, B., Boucherez, J., Briat, J.F., Gaymard, F., and Cellier, F. (2009). Ferritins control interaction between iron homeostasis and oxidative stress in Arabidopsis. Plant J. **57:** 400–412.

Robinson, N.J., Procter, C.M., Connolly, E.L., and Guerinot, M.L. (1999). A ferric-chelate reductase for iron uptake from soils. Nature **397:** 694–697.

Roschzttardtz, H., Conéjéro, G., Curie, C., and Mari, S. (2009). Identification of the endodermal vacuole as the iron storage compartment in the Arabidopsis embryo. Plant Physiol. **151:** 1329–1338.

Salahudeen, A.A., Thompson, J.W., Ruiz, J.C., Ma, H.W., Kinch, L.N., Li, Q., Grishin, N.V., and Bruick, R.K. (2009). An E3 ligase possessing an iron-responsive hemerythrin domain is a regulator of iron homeostasis. Science **326:** 722–726.

Saleh, A., Alvarez-Venegas, R., and Avramova, Z. (2008). An efficient chromatin immunoprecipitation (ChIP) protocol for studying histone modifications in Arabidopsis plants. Nat. Protoc. **3:** 1018–1025.

Schuler, M., Rellán-Álvarez, R., Fink-Straube, C., Abadía, J., and Bauer, P. (2012). Nicotianamine functions in the phloem-based transport of iron to sink organs, in pollen development and pollen tube growth in Arabidopsis. Plant Cell **24:** 2380–2400.

Selote, D., Samira, R., Matthiadis, A., Gillikin, J.W., and Long, T.A. (2015). Iron-binding E3 ligase mediates iron response in plants by targeting bHLH transcription factors. Plant Physiol. **167:** 273–286.

Sivitz, A.B., Hermand, V., Curie, C., and Vert, G. (2012). Arabidopsis bHLH100 and bHLH101 control iron homeostasis via a FIT-independent pathway. PLoS ONE **7:** e44843.

Stacey, M.G., Patel, A., McClain, W.E., Mathieu, M., Remley, M., Rogers, E.E., Gassmann, W., Blevins, D.G., and Stacey, G. (2008). The Arabidopsis AtOPT3 protein functions in metal homeostasis and movement of iron to developing seeds. Plant Physiol. **146:** 589–601.

Thimm, O., Essigmann, B., Kloska, S., Altmann, T., and Buckhout, T.J. (2001). Response of Arabidopsis to iron deficiency stress as revealed by microarray analysis. Plant Physiol. **127:** 1030–1043.

Thomine, S., and Vert, G. (2013). Iron transport in plants: better be safe than sorry. Curr. Opin. Plant Biol. **16:** 322–327.

Toledo-Ortiz, G., Huq, E., and Quail, P.H. (2003). The Arabidopsis basic/helix-loop-helix transcription factor family. Plant Cell **15:** 1749–1770.

Urzica, E.I., Casero, D., Yamasaki, H., Hsieh, S.I., Adler, L.N., Karpowicz, S.J., Blaby-Haas, C.E., Clarke, S.G., Loo, J.A., Pellegrini, M., and Merchant, S.S. (2012). Systems and trans-system level analysis identifies conserved iron deficiency responses in the plant lineage. Plant Cell **24:** 3921–3948.

Valdés-López, O., Yang, S.S., Aparicio-Fabre, R., Graham, P.H., Reyes, J.L., Vance, C.P., and Hernández, G. (2010). MicroRNA expression profile in common bean (*Phaseolus vulgaris*) under nutrient deficiency stresses and manganese toxicity. New Phytol. **187:** 805–818.

Vashisht, A.A., et al. (2009). Control of iron homeostasis by an iron-regulated ubiquitin ligase. Science **326:** 718–721.

Vert, G., Grotz, N., Dédaldéchamp, F., Gaymard, F., Guerinot, M.L., Briat, J.F., and Curie, C. (2002). IRT1, an Arabidopsis transporter essential for iron uptake from the soil and for plant growth. Plant Cell **14:** 1223–1233.

Walker, E.L., and Connolly, E.L. (2008). Time to pump iron: iron-deficiency-signaling mechanisms of higher plants. Curr. Opin. Plant Biol. **11:** 530–535.

Wang, H.Y., Klatte, M., Jakoby, M., Bäumlein, H., Weisshaar, B., and Bauer, P. (2007). Iron deficiency-mediated stress regulation of four subgroup Ib BHLH genes in *Arabidopsis thaliana*. Planta **226:** 897–908.

Wang, L., Ying, Y., Narsai, R., Ye, L., Zheng, L., Tian, J., Whelan, J., and Shou, H. (2013a). Identification of OsbHLH133 as a regulator of iron distribution between roots and shoots in *Oryza sativa*. Plant Cell Environ. **36:** 224–236.

Wang, N., Cui, Y., Liu, Y., Fan, H., Du, J., Huang, Z., Yuan, Y., Wu, H., and Ling, H.Q. (2013b). Requirement and functional redundancy of Ib subgroup bHLH proteins for iron deficiency responses and uptake in *Arabidopsis thaliana*. Mol. Plant **6:** 503–513.

Wellburn, A.R. (1994). The spectral determination of chlorophylls a and b, as well as total carotenoids, using various solvents with spectrophotometers of different resolution. J. Plant Physiol. **144:** 307–313.

Wirstam, M., Lippard, S.J., and Friesner, R.A. (2003). Reversible dioxygen binding to hemerythrin. J. Am. Chem. Soc. **125:** 3980–3987.

Yi, Y., and Guerinot, M.L. (1996). Genetic evidence that induction of root Fe(III) chelate reductase activity is necessary for iron uptake under iron deficiency. Plant J. **10:** 835–844.

Yuan, Y., Wu, H., Wang, N., Li, J., Zhao, W., Du, J., Wang, D., and Ling, H.Q. (2008). FIT interacts with AtbHLH38 and AtbHLH39 in regulating iron uptake gene expression for iron homeostasis in Arabidopsis. Cell Res. **18:** 385–397.

Yuan, Y.X., Zhang, J., Wang, D.W., and Ling, H.Q. (2005). AtbHLH29 of *Arabidopsis thaliana* is a functional ortholog of tomato FER involved in controlling iron acquisition in strategy I plants. Cell Res. **15:** 613–621.

Zhai, Z., Jung, H.I., and Vatamaniuk, O.K. (2009). Isolation of protoplasts from tissues of 14-day-old seedlings of *Arabidopsis thaliana*. J. Vis. Exp. **pii:** 1149.

Zhai, Z., et al. (2014). OPT3 is a phloem-specific iron transporter that is essential for systemic iron signaling and redistribution of iron and cadmium in Arabidopsis. Plant Cell **26:** 2249–2264.

Zhao, M., Song, A., Li, P., Chen, S., Jiang, J., and Chen, F. (2014). A bHLH transcription factor regulates iron intake under Fe deficiency in chrysanthemum. Sci. Rep. **4:** 6694.

Zheng, L., Ying, Y., Wang, L., Wang, F., Whelan, J., and Shou, H. (2010). Identification of a novel iron regulated basic helix-loop-helix protein involved in Fe homeostasis in *Oryza sativa*. BMC Plant Biol. **10:** 166.